CHANNELING RADIATION

(溝道輻射)

BY

HUI YUK TAK

(許育德)

A THESIS SUBMITTED

IN PARTIAL FULFILMENTS OF

THE REQUIREMENTS FOR THE DEGREE OF DOCTOR OF PHILOSOPHY

IN PHYSICS

THE CHINESE UNIVERSITY OF HONG KONG

(1987)

C O N T E N T S

LIST OF TABLES

LIST OF FIGURES

ACKNOWLEDGEMENT

I would like to express my deep gratitude to my supervisors Professor Y.W. Chan and Dr. K. Young for their guidance and supervision.

Thanks are also due to Miss Nancy Hui and Miss S.N. Kung for their help to prepare this manuscript.

The financial support of the Institute of Science and Technology of the Chinese University of Hong Kong is cordially acknowledged.

ABSTRACT

The main characteristics of radiation by channeled relativistic charged particle is briefly reviewed. Radiation due to the periodicity of the crystal potential along the transverse planar direction is studied in detail for positron channeling. This radiation, which we call coherent line bremsstrahlung, may be comparable to the Channeling Radiation and is tunable by rotation of the crystal. The photon energy of this effect is proportional to the square of the energy of the incident particles.

INTRODUCTION

The basic idea that the radiation of a relativistic charged particle with velocity v moving in a periodic structure which forces the particle to oscillate with frequency ω_o in the laboratory will shift the photon energy emitted by the particle to $2\gamma^2\omega_o$ (see section 2.1) leads to several studies of tunable radiation. These novel sources of radiation can be based on charged particle interactions with different periodic structures. The structure could be realized by a periodic magnetic field, a high intensity laser (free electron lasers) or even a metallic diffration grating (Smith, Purcell-Salisbury effect). The wavelength of radiated photon by a typical free electron laser, which has a magnetic field of a 3.2cm period and 43 MeV electron, is 3.4μm.[Deacon, et al., 1977]. That by the Smith, Purcell-Salsibury effect, with a grating of 8000 grooves per cm, and electron beam of 300 keV, is 5000A. [Smith and Purcell, 1953]

If a crystal serves as an interaction structure, the situation is complicated, because in a crystal different aligned incidence or different type of charged particles produce different characteristic electromagnetic radiation. In the early 1950's H. Uberall [Uberall, 1956] discussed the coherent bremsstrahlung (C.B. effect) produced by charged particles on crystal. In studying the physical phenomena of energetic charged particles incident upon a solid target, with direction close to a major crystal axis or crystal plane, high transimission was found. This effect was discovered in measurement and calculation of ion range in crystals. It was also shown that this channeling effect is not only possible for ions but also for relativistic charged

leptons [Andersen, Augstyniak, 1971; Anderson, Bell et al., 1973] . In a series of publications by Kumakhov et al. [Kumakhov, 1977; Kumakhov and Wedell, 1977; Kumakhov and Trikalinos, 1980] based upon these ideas, a new physical effect called channeling radiation (C.R. effect) or Kumakhov effect was predicted. Kumakhov stated that the crystal field would force the channeling charged particles to radiate at a high energy (33 keV for particle energy of 56 MeV). This prediction of Kumakhov as confirmed not only by more detailed theoretical considerations but also by experimental results [Alguard et al., 1979].

The main difference between C.B. and C.R. is that the frequency of C.B. depends on the periodic structure of crystal while the frequency of C.R. depends on the oscillating frequency between atomic planes or atomic strings. It was shown that C.B. effect is suppressed under channeling conditions and the peak power of C.B. radiation is smaller than that of Kumakhov radiation. However, we find that under certain particular conditions, the radiation due to periodic interaction of channeled particle, which we call coherent line bremsstrahlung, is comparable to the Kumakhov radiation. This effect is always neglected in the usual planar approximation. The frequency due to this effect is tunable by rotation of the crystal. For 50 MeV incident positron, the radiated photons have typical energies of 0.5-1 MeV.

In this thesis we shall give a brief introduction of the channeling radiation and discuss the coherent line bremsstrahlung.

1. Channeling Effect

The channeling effect can be qualitatively understood as follow:

If the direction of a charged particle incident upon a crystal is close to a major crystal direction, the particle will suffer small-angle scattering with high probability as it passes through the first layer of atoms. This first deflection will be small enough so that the particle will suffer a similar small-angle deflection at the next layer. Because of the ordered structure of the crystal, the particle will undergo a correlated series of small-angle collisions. This result causes such particles to follow trajectories which oscillate to and fro in the "channels" between atomic rows and planes.

This channeling effect of heary ions has been studied in great detail and proved to be an essential tool for the studies of the surface of solids, radiation damage in single crystals; furthermore, the effect has been used in the area of semiconductor physics for determining the lattice location of dopant atoms and annealing behaviour [Gemmell,1974].

1.1 The Continuum Potential Model

In the analysis of channeling effect, since the deflection angles of the charged particles through the crystal are very small, the momentum transfer to the particle, which is nearly perpendicular to the direction of motion, can be evaluated in the impulse approximation from the interaction of a single collision (Fig.1.1)

$$\delta\vec{P}_{\perp} \simeq -\int_{-\infty}^{+\infty} \frac{dz}{v_{\parallel}} \vec{\nabla} V \qquad (1.1.1)$$

where V is the potential of the particle-atom interaction, z is the direction of motion and V_{II} is the longitudinal velocity of the particle. The momentum transfer in Eq.(1.1) can be determined by the integrated transverse force, which may be obtained from the continuum string potential smeared in the z direction

$$U_{string}=\frac{1}{d}\int_{-\infty}^{+\infty} dz\, V \qquad (1.1.2)$$

Similarly, for a particle channeling between planes, the motion is in effect governed by a continuum planar potential

$$U_{plane}^{(y)}=n\int_{-\infty}^{+\infty} dx\,dz\, V(x,y,z) \qquad (1.1.3)$$

where y is the coordinate perpendicular to the planes, and n is the the areal density of atoms in the plane.

In order to include the effect due to the electron in the crystal. The potential of the single atom should be written as

$$V(r)=\frac{Z_1 Z_2 e^2}{r}\varphi(r/a) \qquad (1.1.4)$$

where $Z_1 e$ and $Z_2 e$ are the charges of the particle and the target nucleus. Respectively, $\varphi(r/a)$ is a screening function of Thomas-Fermi type and a is a screening length. In the Thomas-Fermi theory, the screening length a in Eq.(1.1.4) depends on Z_2 according to the relation

$$= 0.8853 Z_2^{-1/3} a_0 \qquad (1.1.5)$$

where a_0 = 0.53A is the Bohr radius. The Thomas-Fermi screening function cannot be expressed in analytical form. However, there exist several good analytical approximation. The expressions which are most widely used in channeling theory are the ones written by Lindhard [Lindhard, 1965] :

$$\varphi(r/a) = 1 - \left[1 + \left(\frac{\bar{c}\, a}{r}\right)^2\right]^{-\frac{1}{2}} \qquad (1.1.6)$$

where $\bar{C}$ is a standard constant set equal to $\sqrt{3}$. Then, the continuum potential of a string given by Eq.(1.1.2) becomes the Lindhard potential

$$U_{string}(r) = \frac{Z_1 Z_2 e^2}{d} \ln\left[1 + \left(\frac{\bar{c}\, a}{r}\right)^2\right] \qquad (1.1.7)$$

while the potential of a plane by Eq.(1.1.3) becomes

$$U_{plane}(y) = 2\pi Z_1 Z_2 e^2 n \left(\sqrt{y^2 + (\bar{c}a)^2} - y\right) \qquad (1.1.8)$$

Eq.(1.1.8) may be regarded as the first term of a Fourier expansion in x of the periodic potential constructed by Eq.(1.1.7). The coefficients of the succeeding term in general decrease rapidly with distance from the plane and their influences upon the channeled particle averages out close to zero. However we show that under certain conditions this effect cannot be neglected when we consider the electromagnetic radiation of a channeled particle.

1.2 The Critical Angles And The Validity Of The Continuum Potential

In the continuum description of axial channeling, there is a complete separation between the longitudinal motion and the transverse motion. The longitudinal motion has constant momentum while there is conservation of transverse energy

$$E_\perp = \frac{P_\perp^2}{2m\gamma_{||}} + U \qquad (1.2.1)$$

where $\gamma_{||} = 1/\sqrt{(1-(v_{||}/c)^2)}$, $P_\perp$ is the transverse momentum. The additional factor $\gamma_{||}$ in the denominator of the first term is due to the fact that the equation of motion in the transverse plane is given by

$$\frac{d}{dt}\frac{m\vec{v}_\perp}{\sqrt{1-\frac{v_\perp^2+v_{||}^2}{c^2}}} = -\vec{\nabla}U \qquad (1.2.2)$$

If we consider the condition $v_\perp \ll v_{||}$ and $v_\perp/c \ll 1/\gamma_{||}$, Eq.(1.2.2) is equivalent to an equation with rest mass $m\gamma_{||}$, which leads to Eq.(1.2.1)

If the angle of motion relative to the axis is φ , the transverse momentum has magnitude $P_\perp = P\sin\varphi \simeq P\varphi$

The transverse kinetic energy therefore can be written as

$$T_\perp = \frac{1}{2}Pv_{||}\varphi^2 \qquad (1.2.3)$$

For a positive charged particle incident on a string at an angle ψ , the transverse kinetic energy $T_\perp = \frac{1}{2}Pv_{||}\psi^2$, if this kinetic energy is less than the potential energy

at the centre of the string, the particle cannot penetrate to the centre. Since the continuum potential barrier is of order

$$\frac{Z_1 Z_2 e^2}{d} \qquad (1.2.4)$$

the critical angle at which the particle just cannot reach the string is approximately equal to Lindhard's characteristic angle , given by

$$\psi_1 = \left(\frac{4Z_1 Z_2 e^2}{dPV}\right)^{1/2} \qquad (1.2.5)$$

The potential barrier of a plane given by Eq.(1.1.8) is of order

$$\frac{Z_1 Z_2}{d_1}\left(\frac{\bar{c}a}{d_2}\right) \qquad (1.2.6)$$

where the and in Eq.(1.2.6) are the separations of atoms on the plane. Similarly the critical angle of planar channeling is given by

$$\psi_p = \left(\frac{4Z_1 Z_2 e^2}{PVd_1}\right)^{1/2}\left(\frac{\bar{c}a}{d_2}\right)^{1/2} \qquad (1.2.7)$$

The continuum potential approximation is valid when the initial angle of particle incidence with respect to the string or plane is smaller than the corresponding angle given by Eq.(1.2.5), Eq.(1.2.6) or Eq.(1.2.7). Table 1.1 shows typical values of these critical angles of different channels in silicon crystals.

1.3 Applicability Of Classical Description Of Channeling Effect

Most of the channeling effects can be well described within the framework of classical mechanics. In this section, applicability of classical theory is discussed. For classical theory to be valid during scattering from a single atom two conditions must hold

(1) The de Broglie wave-length of the incident particle must be shorter than the range of the interaction.

(2) The diffraction angle due to the uncertainty principle must be smaller than the scattering angle from classical theory. The interaction range is about 1Å to 10Å , thus if the incident particle have momentum greater than $\hbar/1\text{Å}$ to $\hbar/10\text{Å}$, the first condition is fulfilled. If we only consider scattering from a single atom, the classical scattering angle given by Rutheford scattering is

$$\theta_{class} = \frac{2Z_1 Z_2 e^2}{PVb} \qquad (1.3.1)$$

where b is the impact parameter [Jackson, 1975]. The diffraction angle due to the uncertainty principle may be estimated as

$$\delta\theta_{diff} = \frac{\Delta P}{P} = \frac{\hbar}{Pb} \qquad (1.3.2)$$

If the $\sqrt{}$ factor is defined as the ratio of $\theta_{class}/\theta_{diff}$, one may visualize that the classical condition may be written:

$$\nu_R = \frac{\theta_{class}}{\theta_{diff}} = \frac{2Z_1Z_2}{v/c} \gg 1 \qquad (1.3.3)$$

where R denotes the Rutherford scattering and α is the fine structure constant.

For relativistic incident particles, $\nu_R \ll 1$ the classical theory completely loses its validity. This shows that the second condition is violated. However, this is not true for channeled motion considering the case of axial channeling electrons. The classical scattering angle may be estimated as equal to the critical angle given by Eq.(1.2.6) and the uncertainty of position is roughly equal to the screening length a of Eq.(1.1.5). Hence

$$\nu_A = \frac{\theta_{class\ of\ axial\ electron}}{\theta_{diff\ of\ axial\ electron}} \sim \left[\gamma \frac{4a_0}{d} Z_2^{1/3}\right]^{1/2} \qquad (1.3.4)$$

where γ is the Lorentz factor.

Similarly by Eq.(1.2.7) and Eq.(1.2.8), one obtains the ν factors of planar channeling for electrons and positrons, respectively,

$$\nu_p^- \simeq \gamma^{1/2}\left(\frac{4a_0}{d}\right) \qquad (1.3.5)$$

$$\nu_p^+ \simeq \gamma^{1/2} Z_2^{1/3}\left(\frac{2\gamma}{d}\right) \qquad (1.3.6)$$

where 2γ in Eq.(1.3.6) is the planar spacing. The difference between Eq.(1.3.5) and Eq.(1.3.6) is that the position uncertainty of planar channeling

positrons is equal to while that of electrons is given by Eq.(1.1.5). The criterion governing the applicability of classical description is usually given by the number of quantum states available to the channeled particles. Eq.(1.3.4 - 6) is roughly equal to the number of quantum states given by Andersen, Bell et al. [1973]. Owing to the increase of the factors in Eq.(1.3.4 - 6), the classical description is valid for channeled particles having energy much greater than 1 MeV

The channeling effect is roughly classified into two types.

(1) Axial channeling: the main trajectory of the incident follows a string of atoms. Fig.1.2

(2) Planar channeling: the incident particle oscillates to and fro between planes of atoms. Fig.1.3

1.4 Different Types Of Channeling Motion

Different kinds of channeling motion would occur depending on the crystal orientation relative to the incident particle beam. If the particle beam is incident upon a crystal parallel to the atomic string with the beam divergence smaller than the critical angle, then a considerable part of this beam is captured into an axial channel. In axial channeling the electron trajectory can be approximately represented as a spiral winding round the atomic string [Kneiner, et al, 1970]. For a more detailed description of the electron motion the angular momentum conservation law should be taken into account. Therefore, from Eq.(1.2.1) we have

$$E_{\perp} = \frac{P_r^2}{2m} + \frac{L^2}{2mr^2} + U(r) \qquad (1.4.1)$$

where P_r is the radial momentum component, L the angular momentum, and r the radial distance between the electron and the atomic string. The last two terms in Eq.(1.4.1) form an effective potential

$$W(r) = \frac{L^2}{2mr^2} + U(r) \qquad (1.4.2)$$

which has a local minimum, therefore, a bound electron motion around the string become possible for certain incident points ($r_{min} \leq r \leq D/2$, where r_{min} the minimum approach which is possible for an axially channeled particle without dechanneling and D is the distance between the atomic strings in the transverse plane, and incident angles (angles smaller than the critical angle ψ_1). Quantum considerations of axial electron channeling is given in [K.Komaki and F. Fujimoto, 1974].

If the incident beam is not aligned parallel to the atomic string and the tilt angle with respect to crystal planes is smaller than the critical angle ψ_p , the incident particles carry out transverse one-dimensional oscillations. Positive charged particles are repelled from planes and thus oscillate between the middle of two atomic planes. Negatively charged particles are, however, attracted to the atomic planes and cross the planes. For positrons at not too high transverse energies the harmonic potential:

$$V(y) = V_0 y^2 \qquad (1.4.3)$$

with y defined as the distance relative to the mid-plane in the planar channel, is a good approximation. Since electrons experience a potential across the atomic plane, the potential of electron channeling has strong anharmonicity and large potential gradient.

In real experiments, an incident beam of particles is not captured completely into the channeling region. When a particle has transverse energies larger than the value of the potential barrier, it will swiftly pass the atomic planes. This type of motion is called as quasi-channeling.

Different kinds of channeling motion depend on the crystal orientation relative to the incident beam direction. Fig.1.5 shows schematically the tilt-angle regions corresponding to different types of motion. Regions 1 and 2 correspond to axial and planar channeling, respectively. Their boundaries are determined by the corresponding critical angles. Quasi-channeling occurs in regions 4 and 5. Coherent bremsstrahlung (which will be discussed section 5) corresponds to region 6.

2. Characteristics Of Channeling Radiation

The oscillatory motion of channeled particles leads to emission of electromagnetic radiation. As mentioned in section 1.3, classical theory is proper for high energy channeled particles. However, a quantum description is necessary in studying the induced radiation of channeled particles. We now briefly describe the main characteristics of the radiation and introduce both classical and quantum theory of channeling radiation.

2.1 Photon Frequency of Channeling Radiation

We consider a charged particle oscillating transversely with frequency ω_0 during channeling. For energies below the GeV region, the motion is non-relativistic in the co-moving frame, where the essentially uniform translational motion has been transformed away. In the co-moving frame, the particle oscillates at frequency $\gamma\omega_0$ owing to time dilation, and it radiates at this frequency (and higher harmonics) with the angular distribution characteristic of a dipole radiation. A Lorentz transformation back to the laboratory frame gives the photon frequency

$$\omega = \frac{\gamma\omega_0}{\gamma(1-\beta_{\parallel}\cos\theta)} \simeq \frac{2\gamma^2\omega_0}{1+(\gamma\theta)^2} \qquad (2.1.1)$$

where θ is the angle between the beam and the direction of observation of the radiation in the laboratory frame.

At $\theta = 0$, Eq.(2.1.1) gives the maximum frequency

$$\omega_m = 2\gamma^2\omega_0 \qquad (2.1.2)$$

In the case of free electron lasers, ω_0 is independent of γ. However, this is not true in channeling radiation. Following the discussion by Kumakhov [1976], the interaction of a relativistic positron moving in a planar channel can be taken as a harmonic potential by Eq.(1.4.2). Then the equation of motion in the transverse plane is given by

$$\frac{d}{dt}\frac{mV_y}{\sqrt{1-\frac{V_y^2+V_z^2}{c^2}}} = -2V_0 y \qquad (2.1.3)$$

If we consider $V_y \ll V_z$ and $V_y/c \ll 1/\gamma$ (dipole approximation), the equation can be approximated as

$$\ddot{y} = -\frac{2V_0}{m\gamma} y \qquad (2.1.4)$$

where $\gamma = 1/\sqrt{1-V_z^2/c^2}$

This shows that the oscillation frequency of Eq.(2.1.4) is given by

$$\omega_0 = \omega_{00}\gamma^{-\frac{1}{2}} = \sqrt{\frac{2V_0}{m}}\gamma^{-\frac{1}{2}} \qquad (2.1.5)$$

where ω_{00} is the usual frequency of a simple harmonic oscillator. From this it follows that the maximum frequency of positron channeling radiation is

$$\omega_m = 2\gamma^{3/2}\omega_{00} \qquad (2.1.6)$$

whereas in the case of free electron lasers $\omega_m \propto \gamma^2$. However, since the fields are very strong in crystals, one gets a very high value of ω_{00} and therefore the maximum frequency ω_m of Kumakhov radiation is many orders higher than the corresponding frequency in free electron lasers.

2.2 Radiation Spectrum

The most convenient way to discuss the radiation of a charged particle with charge e moving in the direction with average velocity V_{11} and oscillating with frequency ω_0 is to consider the radiation in the co-moving frame of the charged particle.

As mentioned in the preceding section, owing to time dilation, the oscillation frequency as seen by the particle in the co-moving frame is

$$\gamma_{11}\omega_0 \qquad (2.2.1)$$

and the particle can radiate only at frequencies that are integral multiples of $\gamma_{11}\omega_0$. Under the dipole condition discussed in section 2.1, the radiation of the particle has the characteristic of dipole radiation. In the co-moving frame, the radiation of each harmonic is monochromatic (the line width being negligible). The radiation intensity per unit frequency and unit solid angle of harmonic n in the co-moving frame is given by

$$\frac{dI}{d\Omega' d\omega'} = \frac{e^2}{4\pi c^3}|\vec{a}_{\perp n}|^2 \sin^2\Theta\, \delta(\omega' - n\gamma_{11}\omega_0) \qquad (2.2.2)$$

where the $\vec{a}'_{\perp n}$ is the Fourier components of the acceleration given by $\vec{a}'_{\perp n}=\frac{1}{T}\int_0^T \vec{a}(t)e^{\frac{i2\pi n}{T}}dt$,

ω' is the frequency of the radiation and θ' is the angle between $\vec{a}'_{\perp n}$ and the direction of observation (Fig.2.1). The primed quantities are those in the co-moving frame. The delta function is a direct consequence of the monochromatic nature of the dipole radiation. However, when Eq.(2.2.2) is transformed into the laboratory frame, owing to Eq.(2.1.1), we find that at different angles in the laboratory frame, the radiation has different frequencies. Integrating the transformed equation over angles yields the power spectrum

$$\frac{dI}{d\omega}=\frac{3I_n}{\omega}F\left(\frac{\omega}{\omega_m}\right) \qquad (2.2.3)$$

where $F(\xi)=\xi(2\xi^2-2\xi+1)\theta(1-\xi)$

in which θ is the unit step function.

The maximum frequency ω_m in Eq.(2.2.3) corresponding to emission in the forward direction is given by Eq.(2.1.2) or Eq.(2.1.6) and I_n denotes the total power of radiation of harmonic n . For different harmonics, ω_m has different integral multiples of $2\gamma_{\parallel}^2\omega_0$ or $2\gamma_{\parallel}^{3/2}\omega_{00}$. If the potential is not too far from being harmonic, we expect a strong predominance of the lowest frequency in the radiation spectrum (n=1) while for a strongly anharmonic potential, several higher harmonics appear in the spectrum in addition to the first one. The angular distribution in the laboratory following the general character of relativistic particle radiation, i.e. the

main part of intensity is emitted within the angle $1/\gamma$.

2.3 Positron Channeling Radiation

For the case of positron channeling, the spectral and angular distribution of radiation intensity were calculated under dipole approximation by Kumakhov [1977]. Since the potential is approximated as a harmonic potential, the first harmonic predominates in the spectrum. The total intensity is given by

$$I = \frac{e^2 y_0^2 \omega_0^4 \gamma_{11}^4}{3c^3} = \frac{e^2 \omega_{00}^2 \gamma_{11}^2 y_0^2}{3c^3} \qquad (2.3.1)$$

Hence, it is seen that the radiation increases as γ_{11}^2 or E^2 .

Fig.2.2 shows a typical spectrum for positrons. We can see a sharp maximum at $\omega = \omega_m$, which means that the radiation is quite monochromatic. Because of the one dimensional transverse motion, the radiation is linearly polarized.

The influence of the line broadening mechanisms and the potential anharmonicity have been investigated by Pantell and Alguard [1979]. The line broadening mechanisms lead to a full width at half maximum of 13%.

2.4 Electron Channeling Radiation

In the case of electron channeling, the particles undergo a periodic motion across the atomic planes. Therefore the interaction potential between the atomic plane is highly anharmonic and the oscillation frequency depends on the distance of electron relative to atomic planes. In comparison with the properties of positron radiation in planar channeling, we find the following

characteristic features of electron radiation in planar channeling.

(1) The electron radiation should have a broader spectrum than the positron radiation because of the strong potential anharmonicity.

(2) The electron radiation exceeds roughly by one order of magnitude the intensity of positron radiation because the potential gradient of electron channeling is larger than that of positron channeling.

(3) Since the oscillation frequency depends on the distance of electron relative to the atomic plane, the oscillation frequency takes on several different values. Therefore the spectrum exhibits several peaks. A typical spectrum is given by Fig.2.3. [Berman et al, 1981]

2.5 Axial Channeling Radiation Of Electrons

As mentioned in 1.4 in the case of axial channeling of electron, only a part of the electron beam is captured in the channel. The number of captured electrons is strongly influenced by the beam divergence. The capturing conditions and the beam divergence lead to the appearance of a detailed structure in the radiation spectrum. For a detailed calculation, all these factors should be taken into account. A calculation of the peculiarities in electron axial channeling radiation is given by Bozylev, Glebov and Zhevago [1980]. The main characteristic features of this kind of radiation are as follows:

(1) Because of the remarkable anharmonicity of the electron motion, even in dipole approximation several higher harmonics appear in the spectrum.

(2) The electron channeling radiation which is similar to that of planar channeling exceeds by one order of magnitude than the intensity in the positron case. Furthermore, the radiation frequency is higher than in the positron case at the same particle energy.

2.6 Radiation Under Quasi-channeling Conditions

In real experiments, there also exists the case of quasi-channeling. The radiation of this type of motion is considered by Kumakhov and Trikalinos [1980]. By using the harmonic potential with transverse energies $E_\perp \simeq V_0 d_p^2/4$, where d_p is the channel width, it can be shown that

$$\omega_m^{quasi} = 2\omega_m^{channel}$$

$$\left(\frac{dI}{d\omega}\right)_{quasi} \simeq 0.1\left(\frac{dI}{d\omega}\right)_{channel} \qquad (2.6.1)$$

3. Induced Emission on the Basis of Channeling Radiation

Within a quantal picture, the behaviour of spin-$\frac{1}{2}$ particles is described by the Dirac equation. However, the radiation intensity due to spin magnetic moment is of the order of α^2, where α is the fine-structure constant. The spin effect, therefore, is not important when compared with the dipole radiation, which is only of the order of α. Hence, a simpler Klein-Gordon equation is applied. It is shown that the Hamiltonian of a channeling charged particle can be separated out into longitudinal and transverse parts. If the longitudianl interaction is neglected, the Hamiltonian of the longitudinal part is just the same as that for a free particle moving along the direction of the particle beam. The transverse Hamiltonian is given by the right hand side of Eq.(1.2.1) with $p_\perp$ interpreted as the transverse momentum operater. The classical formulas of dipole radiation can be changed to quantum formulas by replacing y_0^2 in Eq.(2.3.1) with the dipole matrix element $4y_{fi}^2$ and the frequency ω_0 to ω_{fi}, where y_{fi} is the transition matrix of the position operation between the final and initial state of the channeled particle and $\hbar\omega_{fi}$ is the energy different between these two states. The quantal description of channeling radiation can therefore be obtained easily. However, this only corresponds to the spontaneous emission. To consider the possibility of producing a tunable laser by channeling radiation, one must study the induced emission of channeling radiation. The transition probability per unit time for absorption or emission in the co-moving frame is given by the Fermi golden rule. Thus

$$W' = \frac{2\pi}{\hbar} |\langle f|H_I'|i\rangle|^2 \delta(E_f' - E_i - \hbar\omega_{k'}') \qquad (3.1)$$

$$= 2\pi \left(\frac{e}{mc}\right)\left(\frac{2\pi\hbar c}{V'\omega_{k'}'}\right) n_{k\lambda}^{\rightarrow\prime} |\langle f|\vec{P}_{\perp}' \cdot \vec{\varepsilon}_{k'} e^{i\vec{k}'\cdot\vec{x}'}|i\rangle|^2 \delta(\omega_{fi}' - \omega_{k'}') \qquad (3.2)$$

Where $n_{k'\lambda'}^{\rightarrow}$ is the number of photons with momentum $\hbar\vec{k}'$, energy $\hbar\omega'$ and polarization is $\vec{\varepsilon}_{k'\lambda'}^{\rightarrow}$. The primed quantities denote those in the co-moving frame. Under the dipole approximation, one gets

$$W' = \frac{4\pi^2 e^2 n_{k\lambda'}^{\rightarrow}}{\hbar V'\omega_{k'}'c} (\omega_{fi}')^2 |y_{fi}|^2 \sin^2\Theta' \delta(\omega_{fi}' - \omega_{k'}') \qquad (3.3)$$

where Θ' is the angle between the y' direction and the direction of observation. The maximum of the transition probability occurs at $\Theta' = \pi/2$. The flux of incident photons of momentum $\hbar\vec{k}'$ and polarization λ' is given by

$$\text{Flux} = \frac{n_{k'\lambda'} c}{V'} \qquad (3.4)$$

Dividing Eq.(3.4) by this flux gives the cross section

$$\sigma_{fi} = \frac{4\pi^2 e^2}{\hbar\omega_{k'}' c} \omega_{fi}'^2 |y_{+i}|^2 \delta(\omega_{fi}' - \omega_{k'}') \qquad (3.5)$$

Transforming Eq.(3.5) into the laboratory, one obtains the result given by Beloshitskii and Kumakhov [1978]:

$$\sigma_{fi} = \frac{4\pi^2 e^2}{\hbar\omega_{k'}' c} \omega_{fi}^2 |y_{+i}|^2 \delta(\omega - \omega_{fi}) \text{ at } \Theta = \frac{\pi}{2} \qquad (3.6)$$

For a level with a finite width Γ , we must make the subsitution:

$$\delta(\omega-\omega_{fi}) \rightarrow \frac{1}{2\pi}\frac{\Gamma}{(\omega_{fi}-\omega)^2+\frac{1}{4}\Gamma^2} \qquad (3.7)$$

The cross section at the resonance $\omega=\omega_{fi}$ is

$$\sigma_{fi}^{0}=\frac{3}{\pi}\frac{\lambda^2}{\tau\Gamma} \qquad (3.8)$$

Where $\lambda=\pi c/\gamma^2\omega_{fi}$ is the wavelength amplified, and $1/\tau = \frac{e^2|y_{fi}|^2\omega_{fi}^3\gamma^2}{3\hbar c^3}$ is the total probability of the spontaneous transition which can be obtained by the quantal expression of Eq.(2.3.1) divided by $\hbar\omega_{fi}$. τ in Eq.(3.8) is usually interpreted as the life time. The enhancement coefficient G will be equal to $\sigma_{ab}\Delta N_e$ or

$$G=\frac{3}{\pi}\frac{\lambda^2\Delta N_e}{\tau\Gamma} \qquad (3.9)$$

where ΔN_e is the population inversion of the levels of the transverse energy of the beam. The level width Γ is caused by the non-monochromaticity of the beam, multiple scattering, and the band structure due to the periodic arrangement of the channels. The main factor of broadening for positrons with $E \gtrsim 1$ MeV is the multiple scattering ($\tau\Gamma \simeq 100$) . At higher energies the main factor is the non-monochromaticity of the beam. If good mono-chromaticity of the beam ($\Delta E/E < 10^{-4}$) is attained, one can have the radiation width $\tau\Gamma \sim 1$ (at $E \sim 1$ GeV). The working condition for the laser is given by $GL>1$, where L is the amplification length (or the photon range before absorption or scattering). From this condition it follows that at current density $\gtrsim 10^3$ to 10^4 A/cm^2 , it is feasible to provide enhancement in a wide wavelength region up to 100nm .

4. Radiation At Ultra-relativistic Energy

In the preceding sections, our considerations are confined to the dipole approximation i.e. $V_\perp/c \ll 1/\gamma$. At ultra-relativistic velocities the transverse motion in the co-moving frame may be relativistic. The Doppler expression $1-\beta_\parallel$ in Eq.(2.1.1) is usually approximated as

$$1-\beta_\parallel \cos\approx \frac{1}{2\gamma^2}(1+\gamma^2\theta^2) \qquad (4.1.1)$$

In this approximation the contribution of transverse velocity is completely neglected. Now we consider the ultra-relativistic case in which the transverse velocity should be taken into account. Since

$$1-\beta_\parallel^2-\beta_\perp^2=\frac{1}{\gamma^2} \qquad (4.1.2)$$

Therefore

$$1-\beta_\parallel \simeq \frac{1}{2\gamma^2}\left(1+\frac{P_\perp^2}{m^2c^2}\right) \qquad (4.2)$$

With this expression inserted into Eq.(2.1.1), we have photon emission in the forward direction:

$$\omega_m = 2\gamma^2\omega_0(E_\perp)/(1+2\gamma E_\perp/mc^2) \qquad (4.3)$$

where $\omega_0(E_\perp)$, which in general depends on the transverse energy $E_\perp$ for anharmonic potential has the same definition as in Eq.(2.1.5).

For $E_\perp/\gamma mc^2 \gg 1$ one gets $\omega_m \sim \gamma^{1/2}$.

It follows under these conditions for the spectral density at the maximum frequency $\frac{dI}{d\omega} \sim \gamma^{-\frac{1}{2}}$ and in the radiation spectrum higher harmonics appear. Detailed considerations of this effect are presented in Kumakhov and Trikalinos [1980].

As observed in Eq.(4.3), ω_m depends on the transverse energy. Even with a well-collimated particle incident beam, particles still have different transverse energies. Hence the $E_\perp$ dependence of ω_m leads to spectral broadening. However, Ellison, et al. [1982], showed that the anharmonic and non-dipolarity effects combine in such a way that there exists a critical value of the incident momentum at which ω_m becomes practically independent of $E_\perp$. At this momentum a sharp peak in the spectrum is expected. This effect was observed for 5 Gev/c positron at CERN by Atkinson et al. [1982]

5. The Relation Between Channeling Radiation And Coherent Bremsstrahlung

Coherent bremsstrahlung has already been studied for 30 years [Dyson and Uberall, 1955; Uberall, 1956]. A survey of this type of radiation is given by Palazzi [1968]. Since both coherent bremsstrahlung and channeling radiation are due to charged particles interacting with the crystal, Terhune and Pantell [1977] stated that the first Born approximation in calculation of the coherent radiation can be used for explaining the radiation in channeling. However, Greschner and Wedell [1979] showed that coherent bremsstrahlung is suppressed by interference. Anderson et al. [1981] discussed the relation between these two effects. Now we summarize these considerations.

5.1 Classical Argument of Coherent Bremsstrahlung

The theory of coherent bremsstrahlung has some formal complications. It is, however, not very difficult to deduce some important features by using a simple classical argument. Consider a relativisitc charged particle moving along a direction at a small angle with the rows of atoms. When the electron reaches the atom A, it will emit an electromagnetic wave train which propagates along the same direction as the particle. (Fig.5.1) When the particle reaches the atom B, its distance from the beginning of the first wave will be

$$\Delta l = (c - v) l / v \simeq l / 2\gamma^2 \qquad (5.1.1)$$

Where $l = a/\theta$ is the distance from A to B

and $\gamma = 1/[1 - (v/c)^2]^{1/2}$

Therefore, in the new wave emitted at B, the wave with frequency ω will have a phase difference.

$$\Delta\varphi = \frac{\omega \Delta l}{c} \tag{5.1.2}$$

Constructive interference occurs when

$$\Delta\varphi = 2\pi n \tag{5.1.3}$$

where n is an integer number.

From Eq.(5.1.1) to Eq.(5.1.3), one gets

$$\frac{\omega}{c}\,\frac{a}{2\gamma^2\theta_n} = 2\pi n \tag{5.1.4}$$

The difference $\Delta\theta$ between the angles at the m-th and $(m+1)$-th maxima is equal to

$$\Delta\theta = \delta a / 2\pi m(m+1) \tag{5.1.5}$$

where $\delta = \omega / 2\gamma^2 c$

If E = 5 GeV , $\hbar\omega$ = 100 MeV (a case of channeling radiation) one finds $\Delta\theta \approx 10^{-4}/m(m+1)$ which is smaller than the critical angle of channeling. Consequently, a deviation from the initial direction by the influence of the potential of the atomic plane or string leads to an averaging over a great number of maxima and minima of the coherent bremsstrahlung, thereby suppressing amplification by interference.

5.2 Connection Between Planar Channeling Radiation And Coherent Bremsstrahlung

The simplest way to illustrate the connection between planar channeling radiation and the coherent bremsstrahlung is by a classical picture of the motion as shown in Fig.5.2 for electrons passing through a crystal at a small angle to a major plane. The trajectory is governed by correlated collisions with atoms in a plane. This interaction may be obtained by averaging the crystal potential over the two dimensions of the plane as given by Eq.(1.1.3). For angles smaller than the critical angle for channeling, the electron may be captured into a bound state in this transverse potential. The radiation of this electron is the channeling radiation.

For larger angles of incidence, the particle will possess too large a transverse energy to be channeled and will move across the planes and along a straight line. The periodic perturbation of the straight-line by the planar potential will cause emission of radiation. This is coherent bremsstrahlung.

The results of a detailed calculation to demonstrate the relation between the coherent bremsstrahlung and channeling radiation effect by Greschner and Wedell [1979] can be illustrated by the band structure shown in Fig.5.3. (The band structure was obtained by expanding the periodic potential in a Fourier series in y and solved the eignfunctions of the Bloch waves.)

In Fig.5.3, the energy-level diagrams for the three planes are shown. A beam incident at an angle θ to a plane populates only transverse states with a reduced value of the bloch vector ky given by $mrV_z\theta = \hbar(\pm ky + ng)$

where n is an integer and g is $2\pi/dp$

The transverse energy depends only weakly on angle for the low-lying bands (which corresponds to the channeling case), in the opposite limit of high transverse energies (which corresponds to coherent bremsstrahlung case) the states are nearly plane waves and the dispersion relation approaches that for a free particle. Since the potential is symmetric, bound states have a definite parity, and the parity selection rule for dipole radiation only allows transitions with odd Δn . The magnitude of radiation is generally much reduced for $\Delta n > 1$. The dipole transition for high transition energies is small, because neighbouring levels correspond to opposite directions of transverse momentum in an extended zone picture. From this discussion, we know that the radiative transitions can be classified into three types are

(1) bound-to-bound transition which corresponds to channeling radiation.

(2) free-to-bound transition which corresponds to quasi-channeling radiation.

(3) free-to-free transition which corresponds to coherent bremsstrahlung.

6. Coherent Line Bremsstrahlung Of Planar Channeling

Since the potential of atomic planes can be regarded as a sum of the potentials of atomic strings (see Fig.6.1), a planar channeling particle would be subject not only to the average influence of the plane but also to the influence of the periodical collisions with atomic strings. Under this condition, two kinds of radiation can be observed. The first one is the planar channeling radiation; the second one is the coherent line bremsstrahlung (CLB) which is connected with the periodical arrangement of atomic strings. As discussed in the last section, coherent bremsstrahlung of channeling particles are suppressed by interference. It can have significant contribution only when the tilt angle of the incident beam with respect to the plane is much greater than ψ_p given by Eq.(1.2.7) i.e. coherent bremsstrahlung occurs only for unchanneled particles. Hence the appearance of CLB for channeled particles shows the fundamental difference between these two effects. In 1980, Kumakhov and Trikalinos [1980] briefly discussed the CLB effect. They showed that the radiation frequency of CLB effect of planar channeling positron is about an order higher than that of the planar channeling radiation while the intensity of CLB is an order lower. In this section we shall study this effect in detail and show that under an antisymmetric configuration (of atomic planes), in a sense to be made precise below, the enhancement of CLB may be predominant.

6.1 The Interaction Of An Atomic Plane As A Sum of Atomic Strings

The potential seen by axial channeling positron is given by Lindhard's potential Eq.(1.1.7). If the positron has

an incident angle greater than the incident critical angle ψ_1 for axial channeling, the positron will move across atomic strings. Thus the potential of all strings should be taken into account; this gives

$$U(x,y)=\frac{Ze^2}{d}\sum_i \ln\left(1+\frac{\vec{c}^2a^2}{\gamma_i^2}\right) \qquad (6.1.1)$$

where $\gamma_i=(x-x_i)^2+(y-y_i)^2$ and (x_i, y_i) are the transverse coordinates of the strings in the crystal. If the strings are arranged as in Fig.6.1 with spatial periodicity X in the x direction, Eq.(6.1.1) can be expanded in a Fourier series in x .

$$U(x,y)=\sum_{n=1}^{\infty} U_n(y)\cos\frac{2\pi nx}{X} \qquad (6.1.2)$$

where $U_0(y)=\frac{1}{X}\int_0^X U(x,y)dx$

$$U_n(y)=\frac{2}{X}\int_0^X U(x,y)\cos\frac{2n\pi x}{X}dx$$

If Eq.(6.1.1) is applied in the above formulas, we have

$$U_0(y)=\frac{2\pi Ze^2}{dX}\left(\sqrt{y^2+\vec{c}^2a^2}-|y|\right) \qquad (6.1.2a)$$

$$U_n(y)=\frac{2Ze}{ndX}\left(e^{-\frac{2\pi ny}{X}}-e^{\frac{-2\pi n}{X}\sqrt{y^2+\vec{c}^2a^2}}\right) \qquad (6.1.2b)$$

Eq.(6.1.2a) is just the planar potential given by Eq.(1.1.8). The potential given by Eq.(6.1.2b) decribes the periodic interation due to the strings. The force field $\vec{F}=-\vec{\nabla}U$ is given by

$$F_y = \sum_{n=0}^{\infty} A_n \cos \frac{2n\pi x}{X} \qquad (6.1.3)$$

$$F_x = \sum_{n=1}^{\infty} B_n(y) \sin \frac{2n\pi x}{X}$$

where

$$A_n = -\frac{\partial U_n}{\partial y}$$

$$B_n = \frac{2n\pi}{X} U_n \qquad (6.1.4)$$

A_n, B_n in Eq.(6.1.2) are

$$A_0(y) = \mp \frac{2\pi z e^2}{dX}\left(1 - \frac{|y|}{\sqrt{y^2 + \bar{c}^2 a^2}}\right)$$

$$A_n(y) = \mp \frac{4\pi z e^2}{ndX}\left\{ e^{-\frac{2\pi n}{X}|y|} - \frac{e^{-\frac{2\pi n}{X}\sqrt{y^2+\bar{c}^2a^2}}\,|y|}{\sqrt{y^2+\bar{c}^2a^2}} \right. \qquad (6.1.5)$$

where the minus sign is for $y<0$
and the plus sign for $y>0$

6.2 The CLB Effect Of Channeling Positron Under Symmetric Configurations

By using the formulas developed in the last section we study the CLB effect of channeling positron. For channeling positrons, the particles move along the middle of planes, therefore the potential is due mainly to two neighbouring planes. It has its minimum in the centre between atomic planes. Consider two planes arranged as shown in Fig.6.2; the force field of this configuration is given by

$$F_y = \sum_{n=0}^{\infty} f_{yn} \cos \frac{2n\pi x}{X} \qquad (6.2.1)$$

$$F_x = \sum_{n=0}^{\infty} f_{xn} \cos \frac{2n\pi x}{X}$$

where $f_{yn}(y) = A_n(Y-y) - A_n(Y+y)$

$$f_{xn}(x) = B_n(Y-y) + B_n(Y+y)$$

Having expanded $U_n(Y \pm y)$ in a Taylor's series, we find that

$$U_0(Y \pm y) \simeq \frac{2\pi z e^2}{dx}\left(U_0(Y) \pm U_0'(Y)y + \frac{U_0''(Y)}{2!}y^2 + \cdots\right) \qquad (6.2.2a)$$

$$U_1(Y \pm y) \simeq \frac{2ze^2}{d}\left(U_1(Y) \pm U'(Y)y + \frac{U_1''(Y)}{2!}y^2 + \cdots\right) \qquad (6.2.2b)$$

where $U_0(Y) = \frac{2\pi z e^2}{dX}\left(\sqrt{Y^2 + (\bar{c}a)^2} - Y\right)$

$$U_0'(Y) = \frac{2\pi z e^2}{dX}\left(1 - \frac{Y}{\sqrt{Y^2 + (\bar{c}a)^2}}\right)$$

$$U_0''(Y) = \frac{2\pi z e^2}{dX} \frac{(\bar{c}a)^2}{(Y^2 + \bar{c}^2a^2)^{3/2}}$$

$$U_1(Y)=\frac{2Ze^2}{d}\left[e^{-\frac{2\pi Y}{X}}-e^{-\frac{2\pi}{\lambda}\sqrt{X^2+\bar{c}^2a^2}}\right]$$

$$U_1'(Y)=\frac{2Ze^2}{d}\,\frac{2\pi Y}{X}\left[e^{-\frac{2\pi Y}{X}}-\frac{e^{\frac{-2\pi Y}{X}\sqrt{Y^2+\bar{c}^2a^2}}}{\sqrt{Y^2+\bar{c}^2a^2}}Y\right]$$

$$U_1''(Y)=\frac{2Ze^2}{d}\left[\left(\frac{2\pi Y}{X}\right)^2 e^{-\frac{2\pi Y}{X}}-\frac{2\pi Y}{X}\,\frac{Y^2}{Y^2+\bar{c}^2a^2}\,e^{-\frac{2\pi n}{X}\sqrt{Y^2+\bar{c}^2a^2}}\right]$$

Since $\bar{c}a\sim$ 0.33Å, $Y\sim$ 1.0A, $(\bar{ca}/Y)^2\sim$ 0.1 for typical channels in silicons, we can expand the above equation in a power series in $(\bar{ca}/Y)^2$, keeping only the first leading term and subsituting it into Eq.(6.2.1), then the equation of motion for relative small in the co-moving frame can be approximated as

$$m\ddot{y}'=-\gamma k y'\left(1+e_1\cos\frac{2\pi x'}{X}\right) \qquad (6.2.3a)$$

$$m\ddot{x}'=\frac{\pi\gamma R}{X}y'^2 e_1\sin\frac{2\pi x'}{X} \qquad (6.2.3b)$$

where

$$R\sim\frac{4\pi Ze^2}{dX}\,\frac{\bar{c}^2a^2}{Y^3} \qquad (6.2.4)$$

$$e_1\sim 2\left[1+\frac{2\pi Y}{X}+2\left(\frac{\pi Y}{X}\right)^2\right]e^{\frac{-2\pi Y}{X}} \qquad (6.2.5)$$

For $V_x'/c \gg \sqrt{\frac{1}{2}\gamma_R \gamma^2 e}$

(the condition of planar channeling), the term on the right hand side of Eq.(6.2.3b) can be ignored. Eq.(6.2.3b) then gives

$$x' = \gamma \theta_x c t'$$

where θ_x is the angle between the direction of the incident particle and the atomic string in the labooratory. Based upon these approximations the solution of Eq.(6.2.3a) are then

$$y = y_0 \cos(\omega_0' t' + \phi) - \frac{\omega_0'^2 y_0 e_1 \cos\omega_+' t'}{2(\omega_+'^2 - \omega_0'^2)} - \frac{\omega_0'^2 y_0 e_1 \cos\omega_-' t'}{2(\omega_-'^2 - \omega_0'^2)} \qquad (6.2.6)$$

where $\omega_0' = (\frac{\gamma_R}{m})^{1/2}$, $\omega_1' = \frac{2\pi\gamma\theta_x c}{\chi}$, $\omega_\pm' = \omega_1' \pm \omega_0'$ and y_0, ϕ

are determined by initial conditions.

From Eq.(2.3.1), the power radiated in the co-moving frame fequencies ω_0' and $\omega_\pm'$ are

$$P_0' = \frac{1}{3}\frac{e^2}{c^3}\omega_0'^4 y_0^2 \qquad (6.2.7)$$

$$P_\pm' = \frac{1e^2}{3c^3}\omega_0'^4 y_0^2 \left(\frac{\omega_\pm'^2}{\omega_\pm'^2 - \omega_0'^2}\right)^2 e_1^2$$

This shows that

$$\frac{P_0'}{P_\pm'} = \frac{\omega_\pm'^2 - \omega_0'^2}{\omega_\pm'^2}\,\frac{1}{e_1^2} \qquad (6.2.8)$$

In most cases $\omega_{\pm}'^2 \gg \omega_0'^2$, so

$$P_{\pm}' = R_{\pm} P_0'$$

where $R_{\pm} = e_1^2/4$

For a symmetric channels with X = 1.93Å , Y = 0.96Å, $R_{\pm}$ is equal to 0.16. This shows that the intensity of CLB effect is about one order lower than that of the planar channeling Radiation. This result is consistent with that given by Kumakhov et al. [1980].

6.3 The CLB Effect Of Channeling Positron Under Antisymmetric Configurations

Besides the structures considered in the last section, there exists another kind of structure as shown in Fig.6.3, i.e. the lower plane has a shift of with $X/2$ respect to the upper one. The force field now given by

$$F_y = \sum_{n=0}^{\infty} g_{yn} \cos \frac{2n\pi x}{X}$$

$$F_x = \sum_{n=1}^{\infty} g_{xn} \sin \frac{2n\pi x}{X} \qquad (6.3.1)$$

where $g_{yn} = A_n(Y-y) + (-1)^{n+1} A_n(Y+y)$

$$g_{xn} = B_n(Y-y) + (-1)^n B_n(Y+y)$$

The analytic approximations of Eq.(6.3.1) are

$$m\dot{y}' \simeq -\gamma_{ky}' + \gamma_b \cos \frac{2\pi x}{X} \qquad (6.3.2a)$$

$$m\ddot{x}' \simeq -\gamma\frac{2\pi}{X} b y' \sin\frac{2\pi x}{X} \qquad (6.3.2b)$$

where k has the same expression as in Eq.(6.2.4) and

$$b \simeq k\gamma e^{-\frac{2\pi\gamma}{X}}\left(1+\frac{2\pi\gamma}{X}\right) \qquad (6.3.3)$$

We note that in contrast to the symmetric cases, we obtain not the type of Eq.(6.2.3), but the equation for the harmonic oscillator deriving by a periodically disturbing force. This difference is due to the fact that at the middle of the atomic planes, the force giving rise to CLB is exactly cancelled out for symmetric channels, while the force for antisymmetric channels is a non-vanishing periodic function. Following the same argument in the last section, we have the solution of Eq.(6.3.2a)

$$y = y_0 \cos(\omega_0' t' + \psi) + \frac{\gamma b}{m(\omega_1'^2 - \omega_0'^2)} \cos\omega_1' t' \qquad (6.3.4)$$

This shows that for the antisymmetric channels, the positron radiates at ω_0' and ω_1'. The coupling terms between ω_0' and ω_1' do not appear under this approximation. The radiated power at ω_0' and ω_1' are respectively

$$P_0' = \frac{e^2}{3c^2}\omega_0'^4 y_0^2$$

$$P_1' = \frac{e^2}{3c^2}\frac{\gamma^2 b^2}{m}\left(\frac{\omega_1'^2}{\omega_1'^2 - \omega_0'^2}\right)^2 \qquad (6.3.5)$$

For $\omega_1'^2 \gg \omega_0'^2$

$$\frac{P_1'}{P_0'} = R_1 \left(\frac{Y}{Y_0}\right)^2 \qquad (6.3.6)$$

Since $\left|y_0/Y\right| \leq$, the ratio

$$R_1 = \frac{b^2}{k^2 Y^2} \qquad (6.3.7)$$

is a measure of the importance of CLB relative to the planar channeling radiation. The important feature for the above discussion is that $P_1'/P_0' \propto y_0^{-2}$, so that P_1' is enhanced for small y_0 at the centre of the channel which has antisymmetric structures. The existence of exponential fall-off of fields in Eq.(6.2.5) and Eq.(6.3.3) show that CLB only can have contribution for narrow planar channel. Fig.6.4 shows the Y/x dependence of R_2 and R_1 .

6.4 The Influence Of Non-nearest Planes

In section 6.2 and 6.3 we only have considered the effect due to the nearest two planes. As shown in Eq.(6.1.2) and Eq.(6.1.5), the terms describing the CLB effect decrease exponentially with the plane distance i.e. the CLB effect is only a short range interaction and therefore can be neglected. The remained influence is due to the planar potential.

Since the distances of these planes which equal to $(2m+1)Y$ (where m are the natural number that greater than unity) are much greater than the oscillating region y , we can used the first term

in Eq.(6.2.2a) to approximate them. Hence, the correction force due to all non-nearest planes is

$$F_{corr} = -\gamma C_S k y' \qquad (6.4.1)$$

where $C_S = \sum_{m=1}^{\infty} \frac{1}{(2m+1)^3} \approx 0.051$

Obviously this correction force would just cause the oscillation frequency to change from ω_0' to $\omega_0'\sqrt{1+C_S}$. The frequency change due to the correction is less than 3%.

6.5 CLB Of Different Channels Of Silicon Crystals

As an example we study the CLB effect of different channel of a single silicon crystal. Silicon crystal used as target in experiment has a diamond structure as shown in Fig.6.5

Its lattice constant is equal to 5.45Å. The atomic number Z = 14 gives a screening length = 0.195Å by Eq.(1.1.5). The string arrangements for the <111> axis and <110> axis are shown in Fig.6.6. The arrangements shown on the figure are end views of the channels. By using these data and the expressions of k, b, c in Eq.(6.2.2) and Eq.(6.3.2), the geometry and typical radiation characteristics are shown in table 6.1 and table 6.2. Channels A and B in table 6.1 have antisymmetric structure as shown in Fig.6.3. Channel D of symmetric structure is shown in Fig.6.4. Channel C shown in Fig.6.7 can be regarded as the superposition of two antisymmetric structure shifted by $\lambda/2$. It can be easily shown that the k and b values are given by Eq.(6.2.3) and Eq.(6.2.4) multiplied by 2 and $\sqrt{2}$

respectively. Table 6.2 indicates that channel A and B is a fairly good channel for the study of CLB effect.

7. Computer Simulation

The equations in Sect.6 are nonlinear. We can only find an analytic approximation for the case of channeling positron of small y. To study the behaviour for large y, we have developed a numerical simulation. All terms higher than $n = 2$ in the force equation in Eq.(6.2.1) and Eq.(6.3.1) are truncated. This approximation is equivalent to neglecting the effect due to the higher harmonics of the CLB effect. To check the validity of this approximation, we have compared this equation with a more "exact" potential field. This "exact" potential field is formed by all strings (shown in Fig.7.1) which have the potential given by Eq.(6.1.1). The transverse force due to this Lindhard's string potential in the co-moving frame is given by

$$\vec{F}_{\perp} = \sum_{All\,i} \frac{2ze^2\gamma}{d} \frac{\bar{c}^2 a^2}{r_i^2(r_i^2+\bar{c}^2a^2)} (\vec{r}_{\perp} - \vec{r}_{\perp i}) \qquad (7.1)$$

Since the direct summation in the above equation coverges slowly (proportionally to $1/r_i$), we calculate the force inside the shadowed region in Fig.7.1 by summing 19 nearest strings (the strings with distance p_i from the centre less than $2X$). The force due to other strings are expanded as power series in r/r_i where $r = \sqrt{x^2+y^2}$ is the distance of the particle from the central string. This correction force is

$$\vec{F}_{corr} = -\frac{2ze^2}{d} r \{c_1 + c_2 (r^2 - \bar{c}^2 a^2)\} \qquad (7.2)$$

where $C_1 = 2 \sum_{p_i > 2X} \frac{1}{p_i^2}$

and $C_2 = 2 \sum_{P_i > 2x} \frac{1}{P_i^6}$

By computer summation, we found that

$$C_1 = \frac{0.672}{X^4}$$

$$C_2 = \frac{0.120}{X^6} \qquad (7.3)$$

Based upon the above equations, the positron motion of all chanels which have the <111> axis as the Z Z-direction can be solved by using the Runge-Kutta method. Fig.7.2a shows the projection in the plane of a typical trajectory of positron moving along the {220} plane. This trajectory was calculated for an initial $y_0 = 0.2\,Y$ relative to the mid-plane, and an angle of 0.523° relative to the <111> axis. In Figs. 7.2b and 7.2c the transverse velocity are also plotted as a function of X along the channeling plane. The Fourier components of the acceleration

$$\vec{a}_n' = \frac{1}{T} \int_0^T dt' e^{-\frac{i2\pi nt'}{T}} \frac{d^2\vec{r}}{dt'^2} \qquad (7.4)$$

are evaluated by Fast Fourier transform method.

Fig.7.2d shows the power spectrum.

$$P' = \frac{2e^2}{3c^3} |a_n'|^2 \qquad (7.5)$$

associated with y and X polarization versus frequency for the same initial condition as used in Figs. 7.2a, b.

All the above calcuation is repeated by replacing the force Eq.(7.1) with the truncated Eq.(6.3.1). Fig.7.3 shows the results. No significant difference between Figs.7.2a, b, c and Figs.7.3a, b, c is found.

The peak which can be found in Fig.7.2d at the second harmonic of the CLB frequency ω_1, disappears in Fig.7.3d. This is due to the fact that the harmonic terms higher than n = 2 are truncated. The agreement of the frequency spectrum lower than $2\omega_1$ between Figs.7.2c, d and Figs.7.3c, d verifies that Eq.(6.3.1) is also a good equation of motion for studying the CLB effect. Since the truncated equation is more convenient and flexible for different channels, we use it to study the channels which the Z axis is not along the <111> axis.

7.1 Simulation Of A Symmetric Channel

As an example of symmetric cases, we have worked out a positron (with $\gamma = 99$, $\theta = 0.512^{\circ}$) moving along channel D. A typical power spectrum with $y_0 = 0.3\gamma$ is shown in Fig.7.4. In the y polarization spectral lines at ω_0 and $\omega_1 \pm \omega_0$ are found. The frequency values are just the same as given by Eq.(6.2.6). In the x polarization, only a spectral line at ω_1 is found. The power intensity of ω_1 is roughly equal to that of $\omega_1 \pm \omega_0$. Hence, the CLB effect would give $\omega_1 - \omega_0$, ω_1, $\omega_1 + \omega_0$ three aditional frequency in the spectrum. However, $\omega_1 \pm \omega_0$ and ω_1 have different polarizations.

For large initial values $y_0 > 0.5\gamma$, the γ frequency peak positions begin to increase. Spectrum of $y_0 = 0.7\gamma$ is shown in Fig.7.5. Besides, the shift of

peak position, new spectral lines due to nonlinear effect appear.

Fig.7.6 shows the radiation intensities as a funciton of initial γ_0 values. The dashed lines are the corresponding power intensity calculated by Eq.(6.2.3.a). We find that for $\gamma_0 < 0.5\gamma$, it is roughly equal to the simulated result.

7.2 Simulation Of An Antisymmetric Channel

Since channel A has an antisymmetric structure, its power spectrum is different from that of channel D. A typical power spectrum has been shown in Fig.7.3d. No coupling terms between ω_0' and ω_1' occurs at the y polarization. At polarizaiton there are two peaks at $\omega_1' \pm \omega_0'$. The simulation also shows that the y polarization dominates: $|a_x'/a_y'|^2 \sim 10^{-3}$.

The relation between the incident angle relative to the <111> axis and the radiated frequency of CLB effect is shown in Fig.7.7 which verifies that $\omega_1 \propto \theta$. The values of ω_1' are equal to that given by the expression in Eq.(6.2.6).

Fig.7.8 shows the radiation intensities as function of initial γ_0 . This figure shows that CLB effect dominates at $\gamma_0 \lesssim 0.3\gamma$. For $\gamma_0 > 0.3\gamma$, CLB effect is smaller than channeling radiation but still has the same order of magnitude.

Fig.7.9 shows the radiation intensities against γ_0 of channel B with $\theta = 0.495^\circ$, $\gamma = 99$. Since channel B is a narrow channel, the enhancement of CLB is greater than that of C.R. for all γ_0 .

8. Discussion And Conclusion

In this thesis, we have given a brief introduction of the main characteristics of channeling radiation. The treatment, which included the interaction due to the periodic arrangement of atomic strings, shows that radiation of frequency $\omega_1' = \frac{2\pi\gamma\theta c}{x}$ appears in the power spectrum. This can be explained as follows: a relativistic charged particle moving in the x - y plane at small angle θx with the Z axis will have a velocity of $\gamma\theta x c$, hence the time period produced by the periodic structure is $x/\gamma\theta x c$ and gives the above oscillation frequency $2\pi\gamma\theta x c/x$. Since this effect is of dipole type, it has a spectral form given by Eq.(2.2.3). This radiation possesses the following properties:

(1) The radiation frequency depends on γ^2 in the laboratory and is proportional to θ. (Hence the photon frequency is tunable by rotation of crystal)

(2) For a symmetric configuration CLB is about an order smaller than the channeling radiation.

(3) In an antisymmetric channel, CLB is always greater than channeling radiation for small y_0 and still has the same order of C.R. when y_0 is larger.

(4) The CLB effect is more significant for narrow channels. We found that there exists at least one channel in which CLB dominates for all y_0 (channel B, see Fig.7.9). The integral power of channel B over all y_0 of CLB is greater than that of channeling radiation about 2.5 times.

The properties that the CLB is polarized to a good degree, and is quite mono-chromatic give the posibility of a wide application like channeling radiation. In

this connection it seems to be necessary to investigate this effect experimentally.

Since CLB can be regarded as an anisotropic effect of the channeling plane (i.e. different incident angles parallel to the plane give different types of radiation), the transition between different axis channeling along the same plane is of great interest. Therefore, further theoretical research should be directed to the development of a general theory which includes the axial channel and CLB effect as special cases.

- END -

References

M.J. Alguard, et al., Phys. Rev. Lett. 42, 1148 (1979)

J.U. Andersen, W.M. Augstyniak and E. Uggerhoj, Phys. Rev. B3, 705 (1971)

J.U. Andersen, F. Bell, F.Frandsen, and E. Uggerhoj, Phys. Rev. B8, 4913 (1973)

J.U. Andersen, E. Bonderup and R.H. Pantell, Ann. Rev. Nucl. Part. Sci. 33 453 (1983)

J.U. Andersen, K.R. Eriksen and E. Laesgaard, Phsica Scripta 24 588 (1981)

M. Atkinson et al., Phys. Lett. B110 162 (1982)

V.V. Beloshitsky and F.F. Komarov, Phys. Reports 93 No.3 117 (1982)

V.V. Beloshitsky and M.A. Kumakhov, Phys. Lett. A69, 247 (1978)

Berman et al., Phys. Lett. A82, 459 (1981)

V.A. Bozylev, V.I., Glebov and N.K. Zhevago, Sov. Phys. JETP 51(11) 31 (1980)

D.A.G. Deacon, et al., Phys. Rev. Lett. 38, 892 (1977)

D.J. Dyson and H. Uberall, Phys. Rev. 99 604 (1955)

D.S. Gemmel, Rev. Mod. Phys. 46, 129 (1974)

Greschner and R. Wedell, Phys. Status solidi (b) 95 B7 (1979)

J.D. Jackson, Classical Electrodynamics (John Wiley, New York-London, 1975)

H.J. Kreiner, et al., Phys. Lett., A33, 135 (1970)

M.A. Kumakhov, Phys. lett. A57, 17 (1976)

M.A. Kumakhov, Phys. status. solidi. (b) 84, 41 (1977)

M.A. Kumakhov, R. Wedell, Phys. status solidi, B84, 581 (1977)

M.A. Kumakhov, Ch. G. Trikalinos, Phys. status solidi, B99, 449 (1980)

J. Lindhard, K. Dan. Vidensk. Selsk. Met. Fys. Medd. 34, N14 (1965)

G.D. Palazzi, Rev. Mod. Phys. V40 611 (1968)

R.H. Pantell and M.J. Alguard, J. Appl. Phys. 50 758 (1979)

S.J. Smith and E.M. Purcell, Phys. Rev. 92, 1069 (1952)

R.W. Tenhune and R.H. Pantell, Appl. Phys. lett. 30, 265 (1977)

H. Uberall, Phys. Rev. 103, 1055 (1956)

Energy (MeV)	Type of channeling	Critical angle
1.5	<110> axial channeling	0.61°
3.0	<100> axial channeling	0.38°
1.5	{110} planar channeling	0.19°
1.5	{100} planar channeling	0.16°

Table 1.1 Typical critical angles of different types of channeled electrons in silicon

	Axis	Plane	Figure	X (Å)	Y (Å)	d (Å)
A	<111>	{220}	6.3	2.23	0.96	4.72
B	<111>	perpendicular to{220}	6.3	3.86	0.56	4.72
C	<110>	{220}	6.7	5.45	0.96	3.85
D	<100>	{220}	6.4	1.93	0.96	5.45

Table 6.1 The geometry of four channels in silicon

	$\hbar\omega_0$ (KeV)	$\hbar\omega_1$ (MeV)	k_{02} (V/A)	b (V/A)	e_1	R_1	$R_\pm$
A	32	.97	33	6.3	-	.04	-
B	48	.56	75	26.1	-	.39	-
C	32	.40	33	12.3	-	.15	-
D	32	.12	33	-	.79	-	.16

Table 6.2 Typical radiation characteristic, assuming E = 51 MeV and = 0.5°

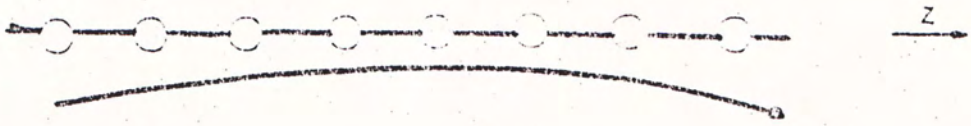

Fig. 1.1 Correlated collisions between incident particles and atoms in a string

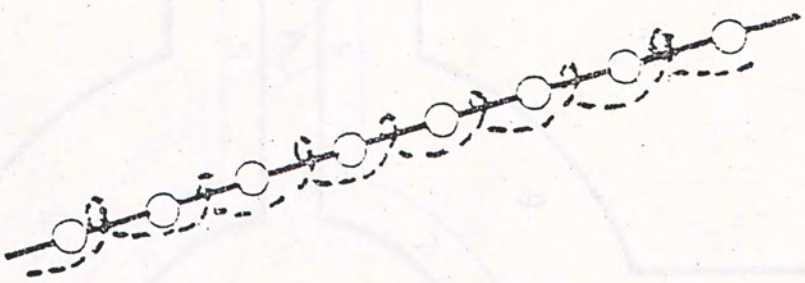

Fig. 1.2 Axial channeling (electron)

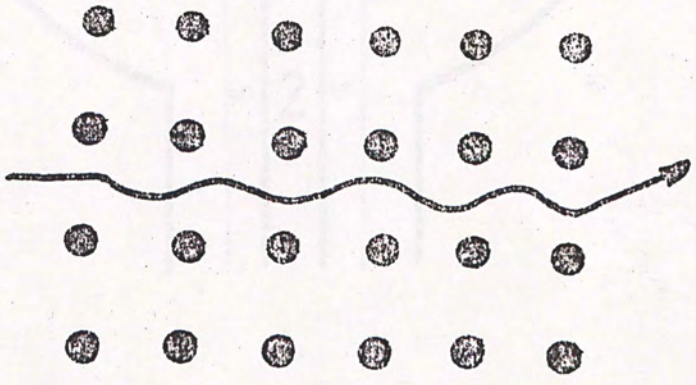

Fig. 1.3 Planar channeling (positron)

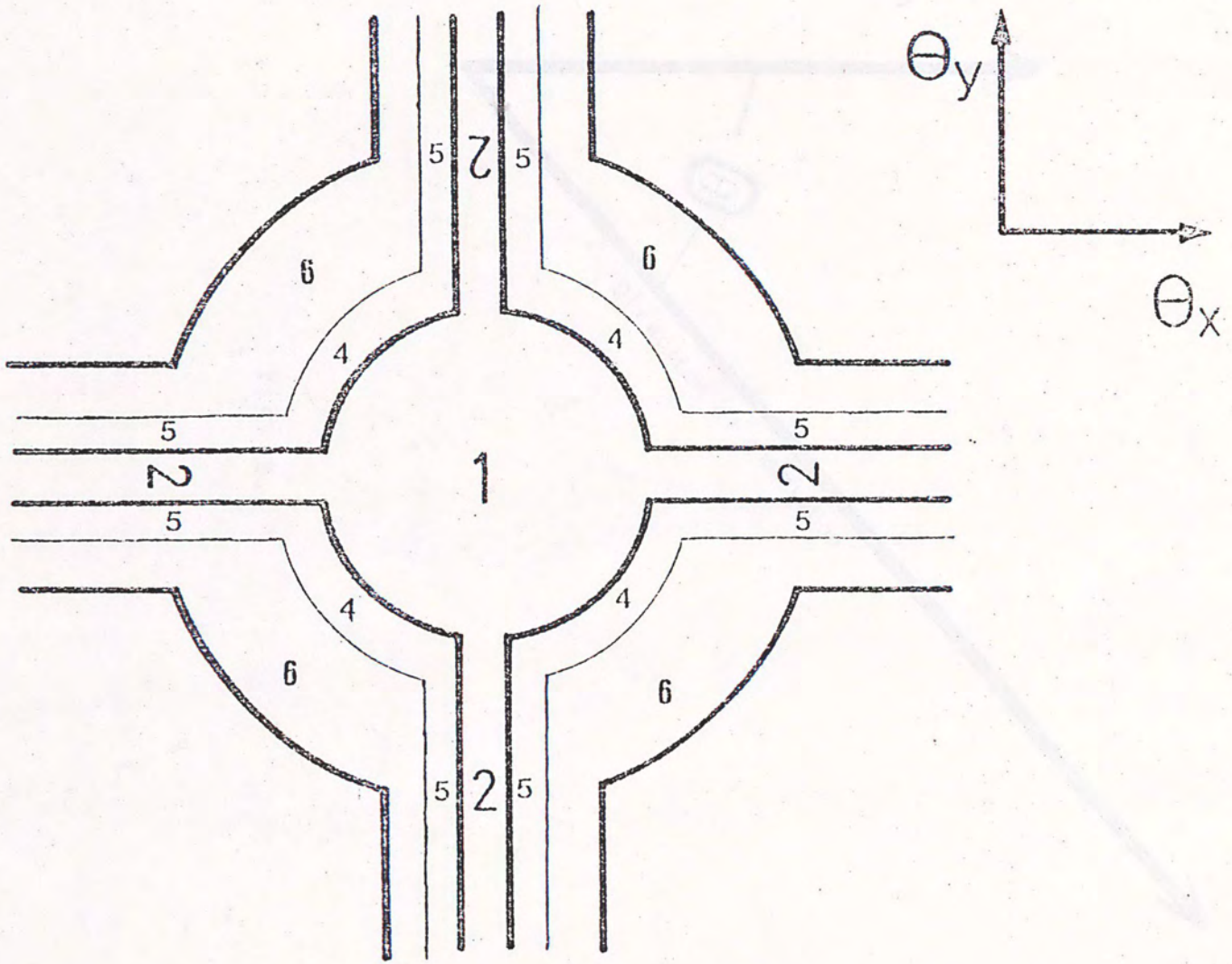

Fig. 1.4 Different kinematic regions

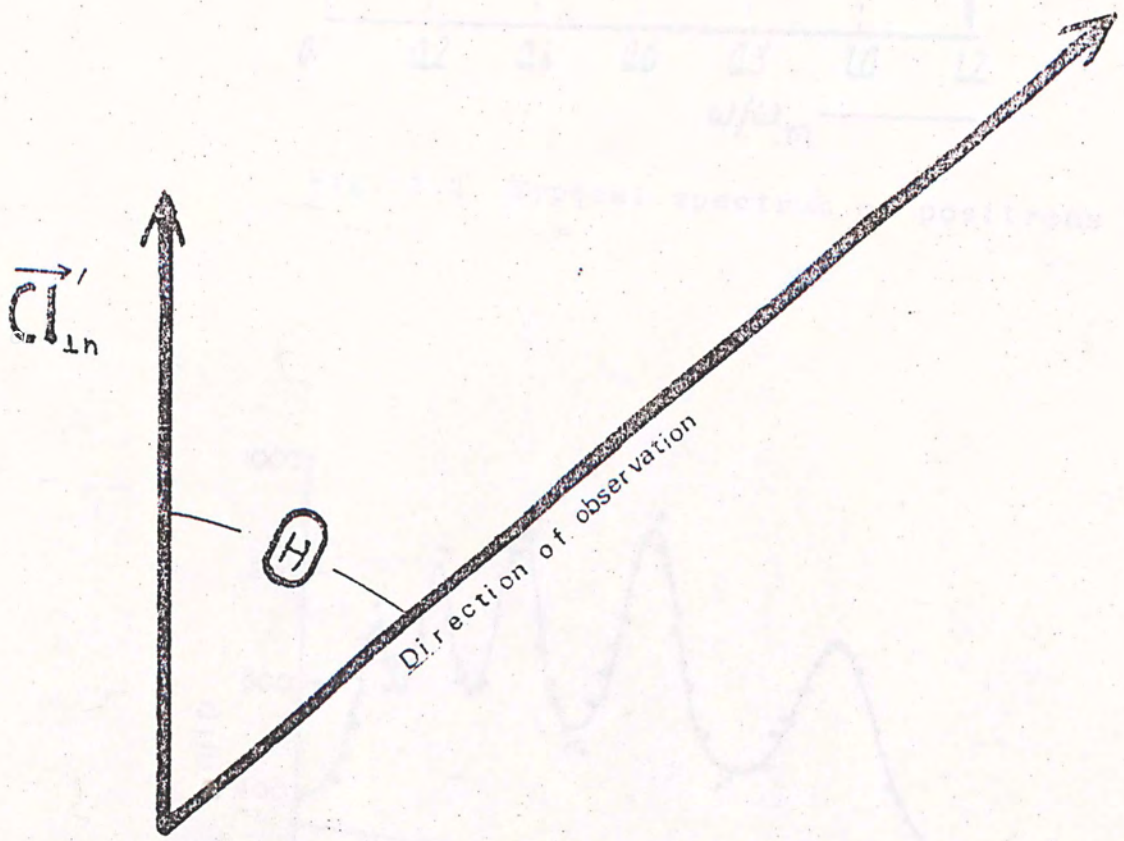

Fig. 2.1

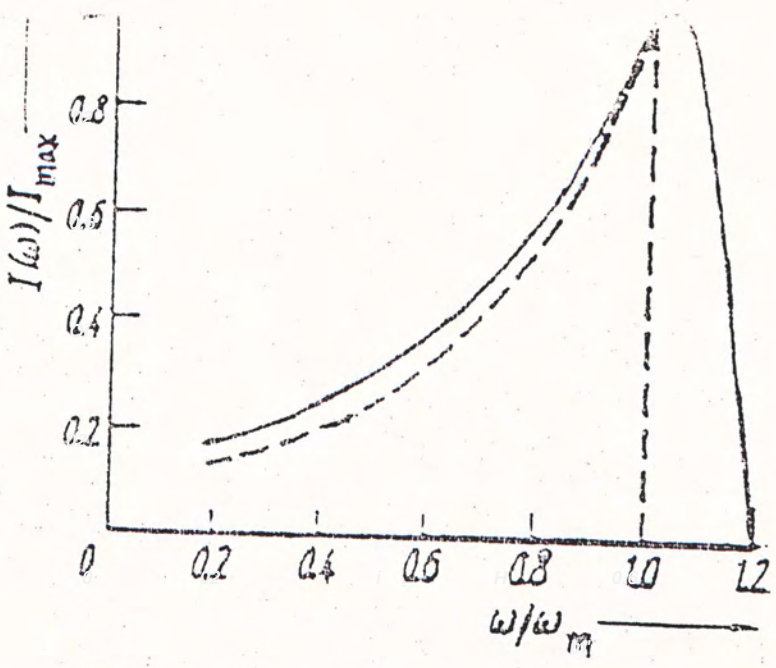

Fig. 2.2 Typical spectrum of positrons

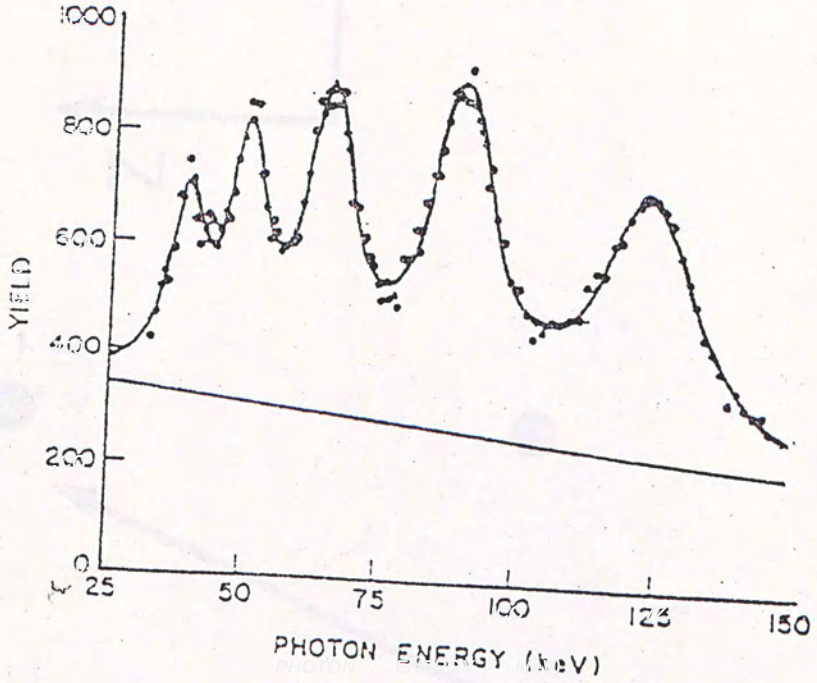

Fig. 2.3 A typical photon spectrum obtained from 54-Mev electrons channeled along {110} plane of a 1.7 m thick Si crystal

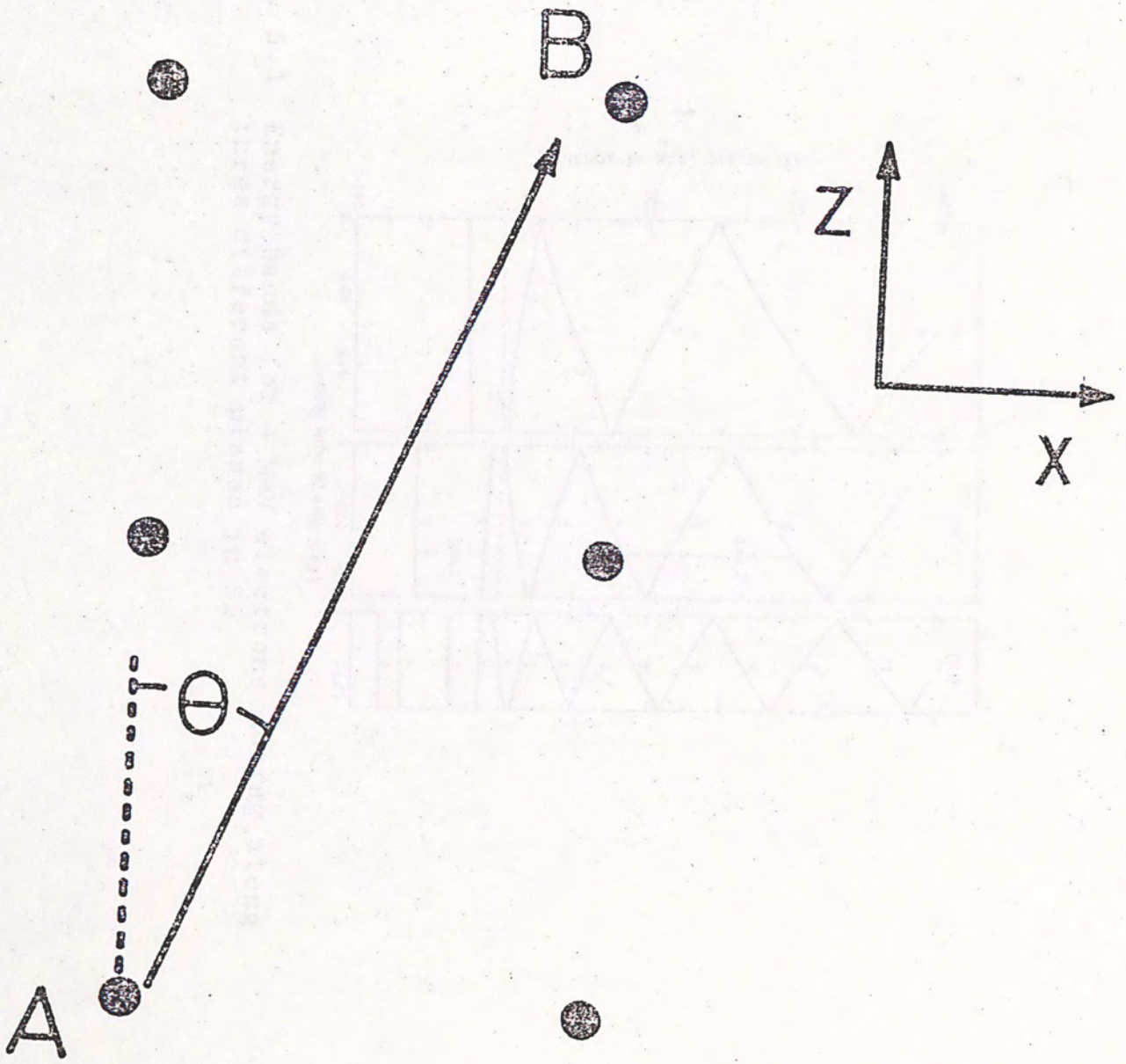

Fig. 5.1 Geometry showing coherent bremsstrahlung

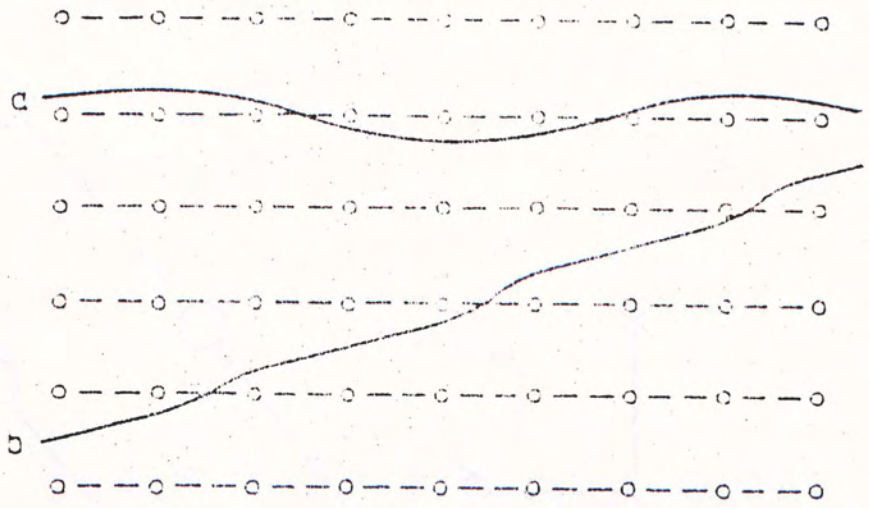

Fig. 5.2 Classical electron motion (a. planar channeling, b. coherent bremsstrahlung)

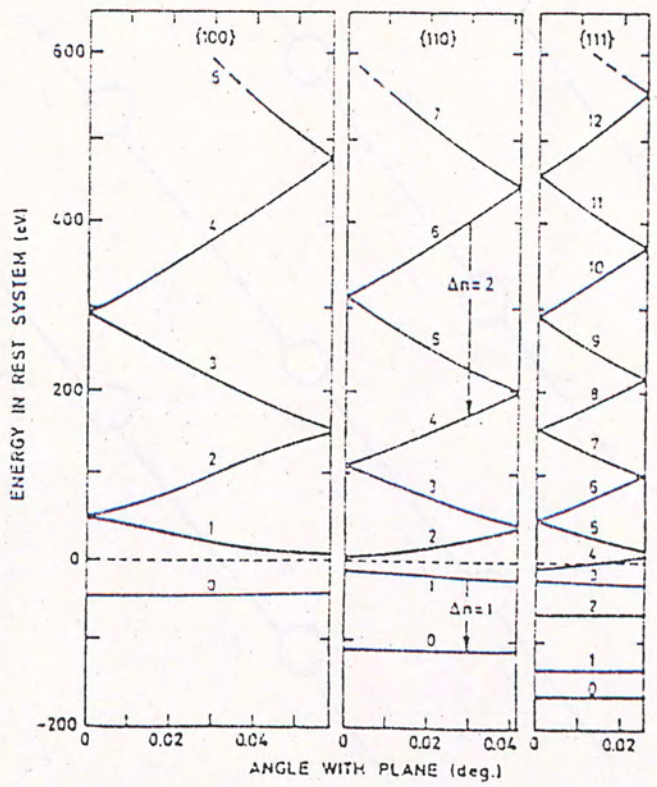

Fig. 5.3 Energy bands for 4 MeV electrons moving along three different planes in Si

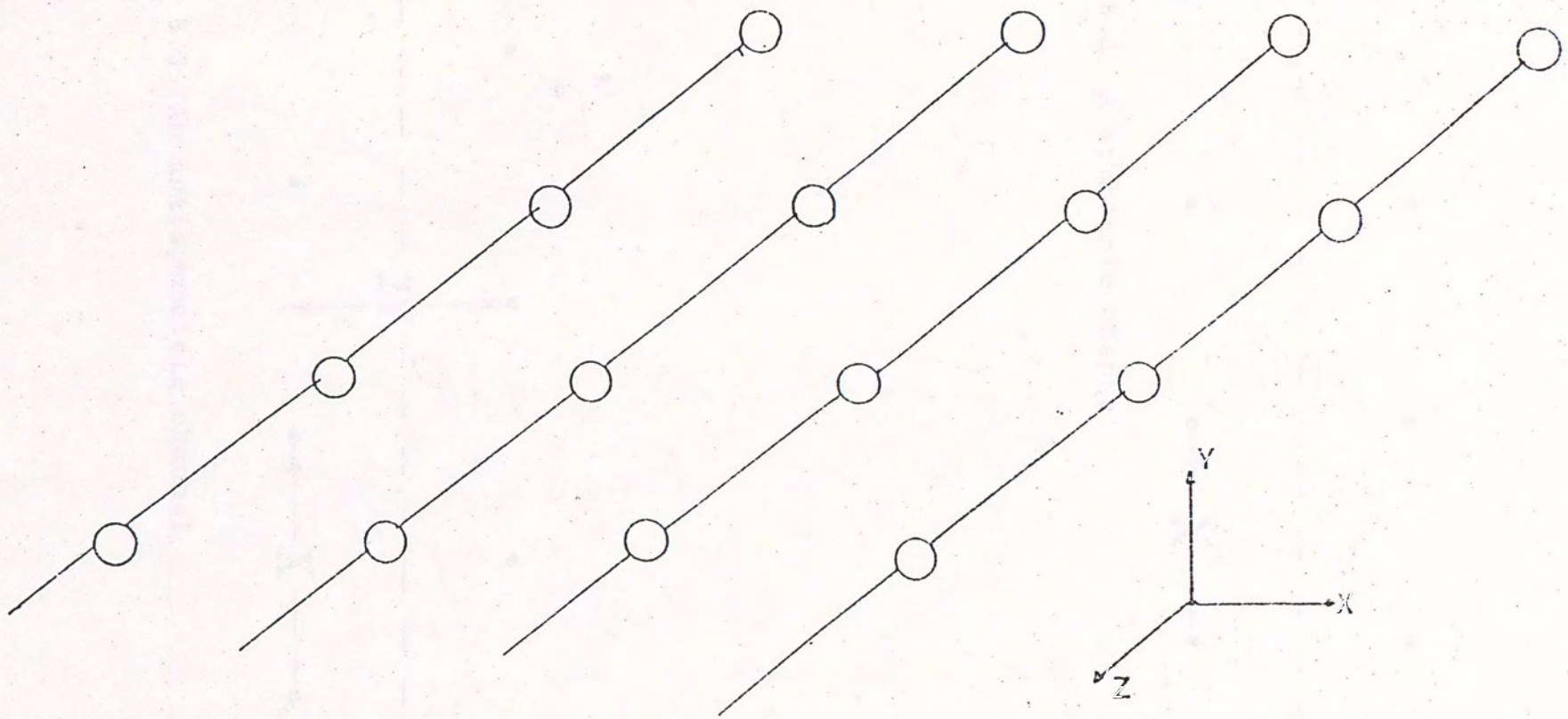

Fig. 6.1

Fig. 6.2 A symmetric channel

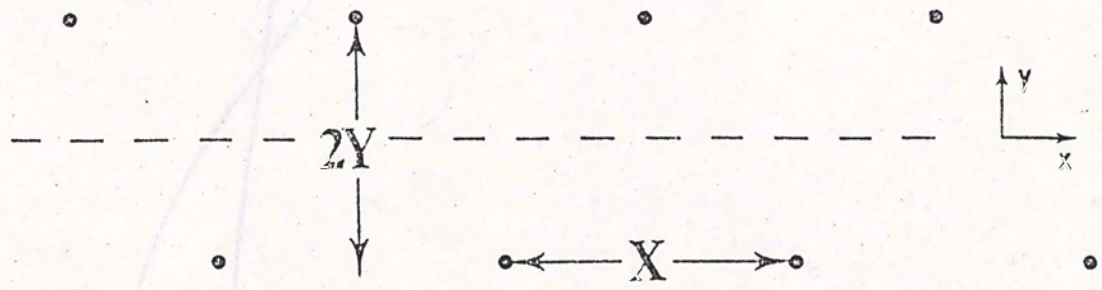

Fig. 6.3 An antisymmetric channel

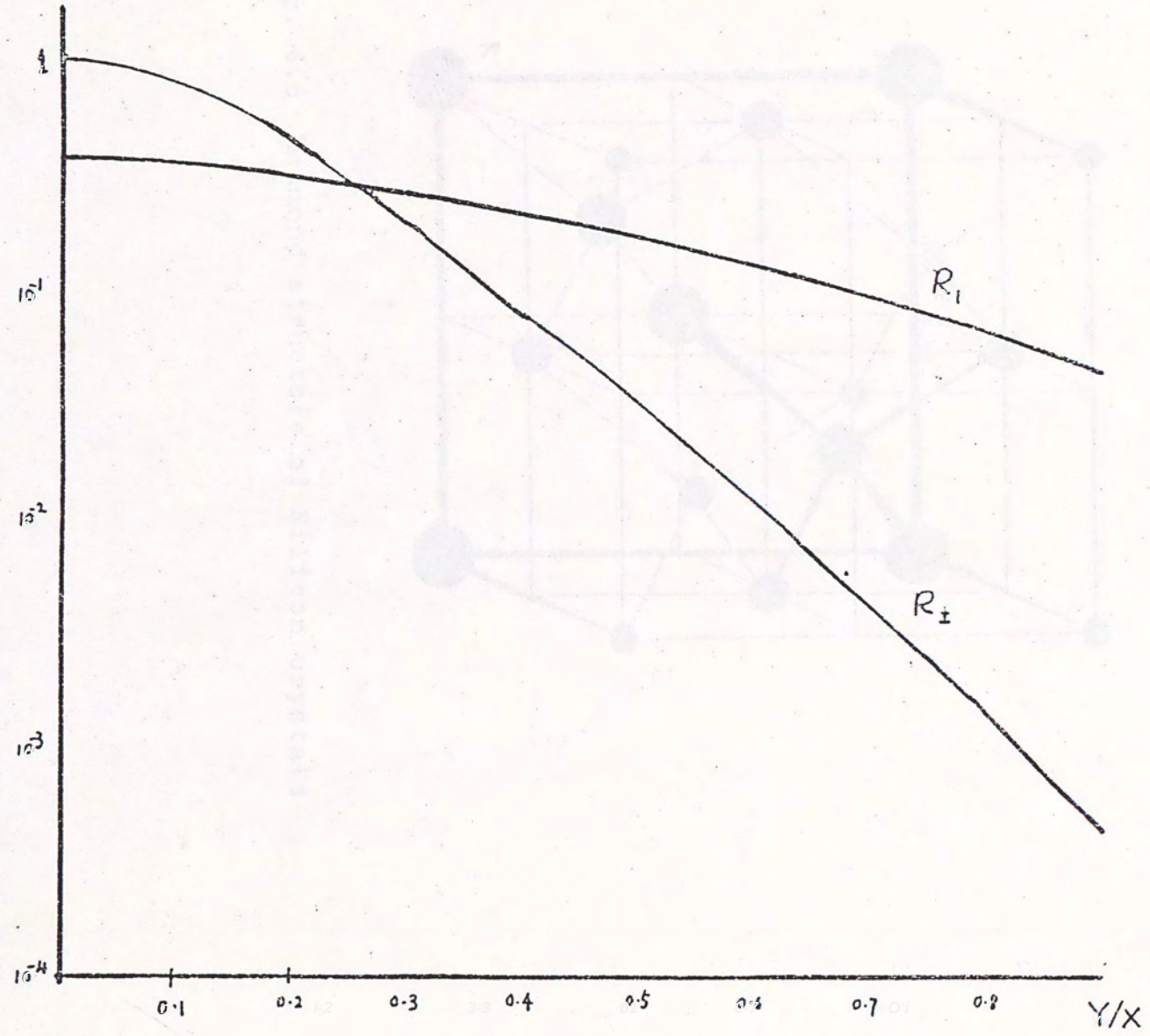

Fig. 6.4 R_1 and $R_\pm$ as a function of Y/X

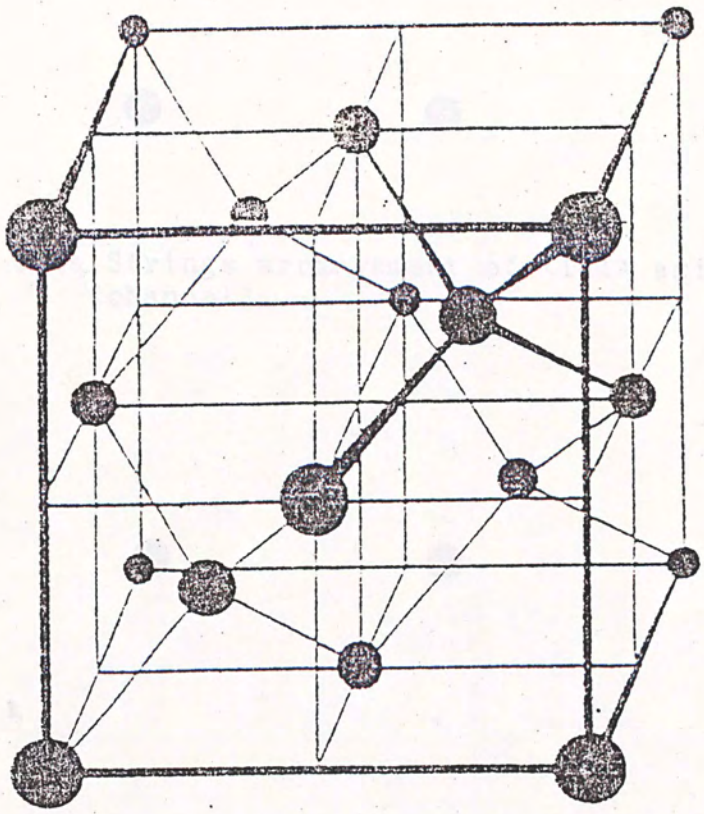

Fig. 6.5 Diamond structure of Silicon crystals

Fig. 6.6a Strings arrangement of <111> axis (end view of the channel)

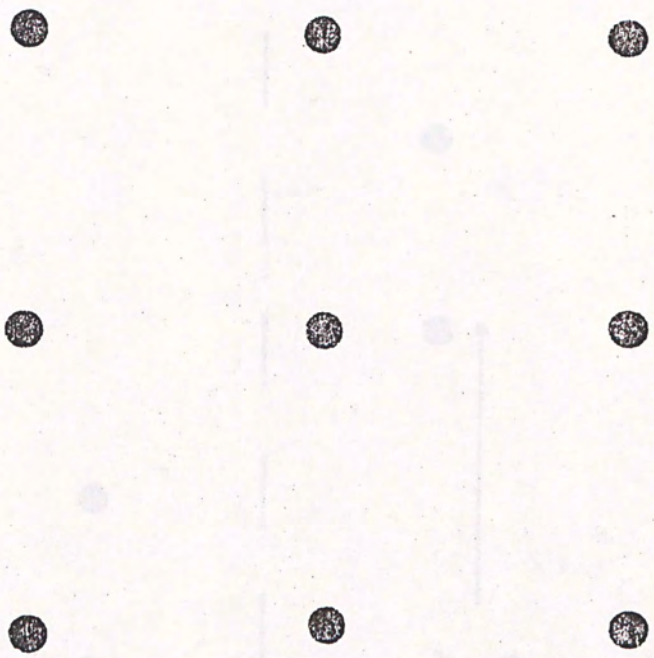

Fig. 6.6b Strings arrangement of <110> axis (end view of the channel)

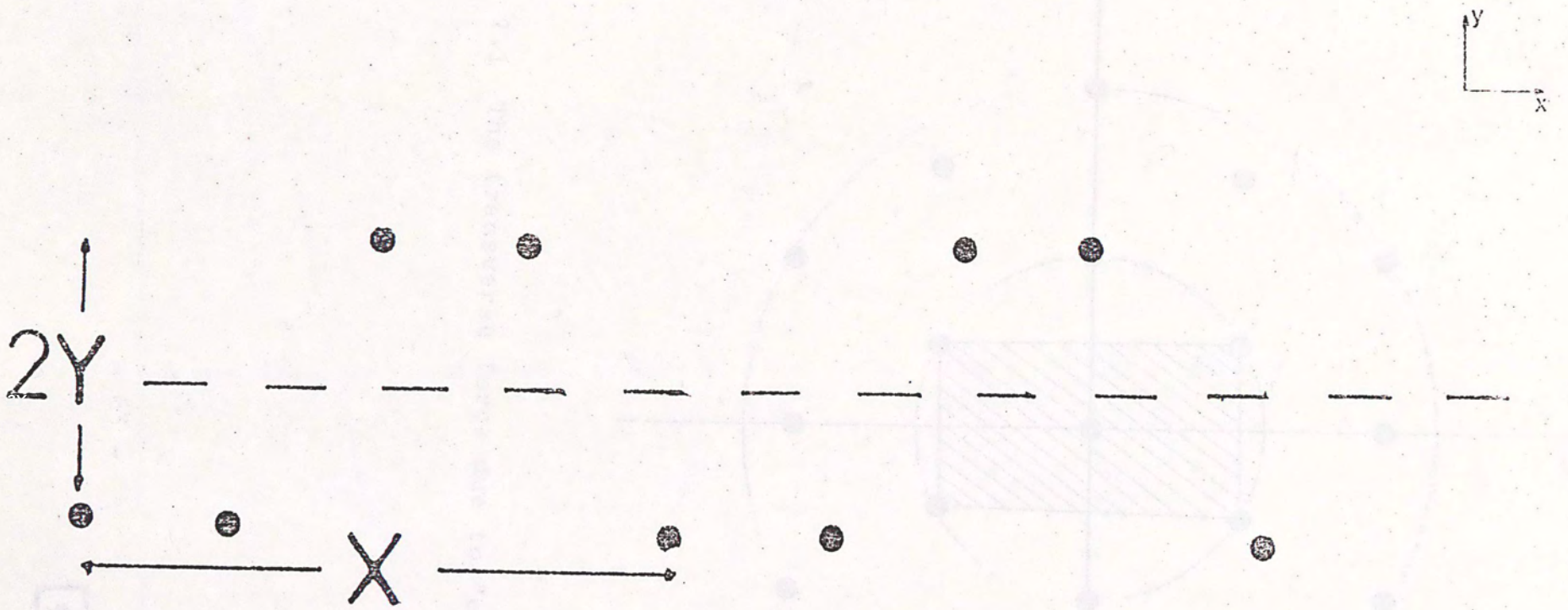

Fig. 6.7 Configuration of channel C

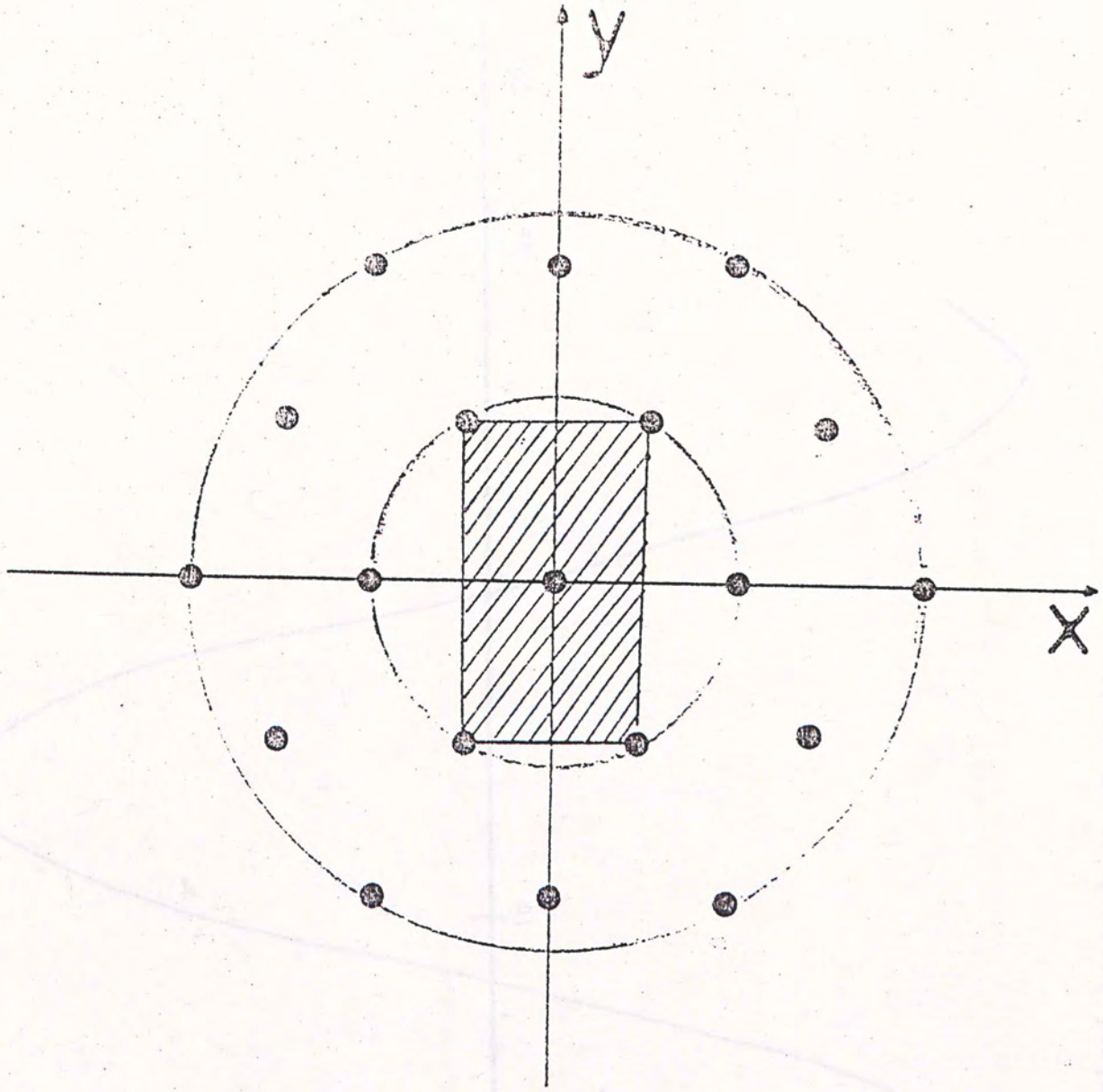

Fig. 7.1 The transverse force due to "exact" potential

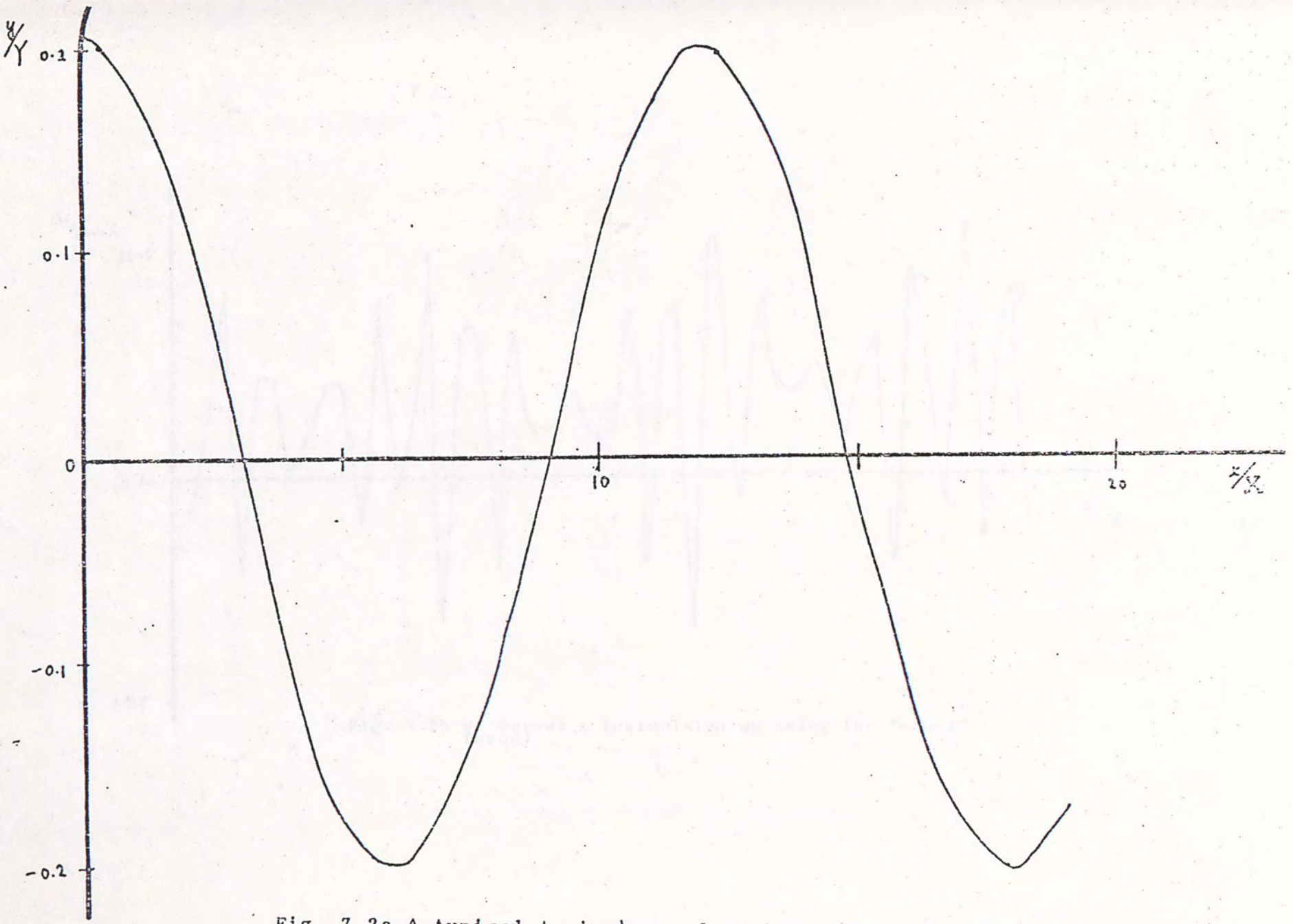

Fig. 7.2a A typical trajectory of positron along the [220] plane (calculated by using the "exact" force)

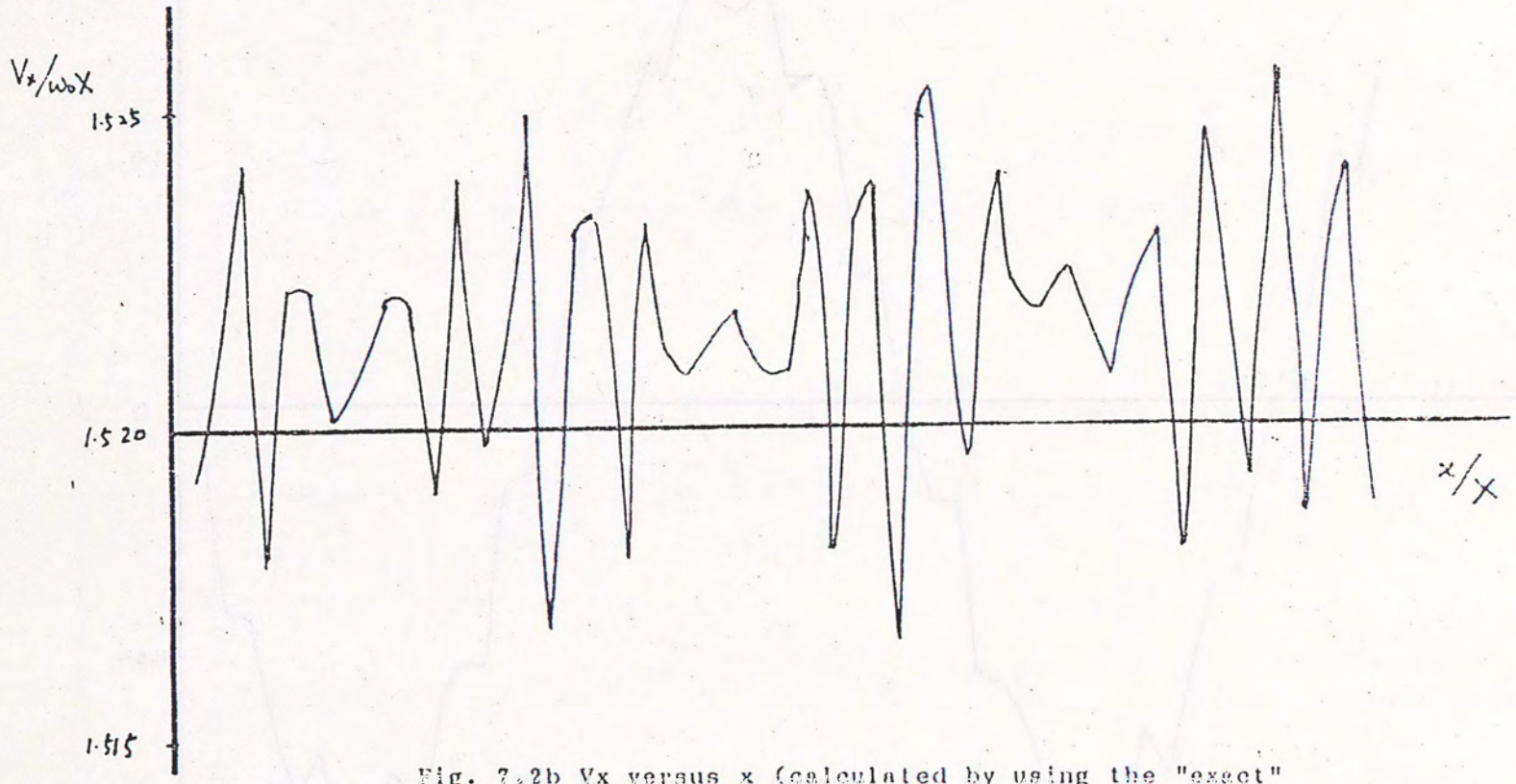

Fig. 7.2b Vx versus x (calculated by using the "exact" force)

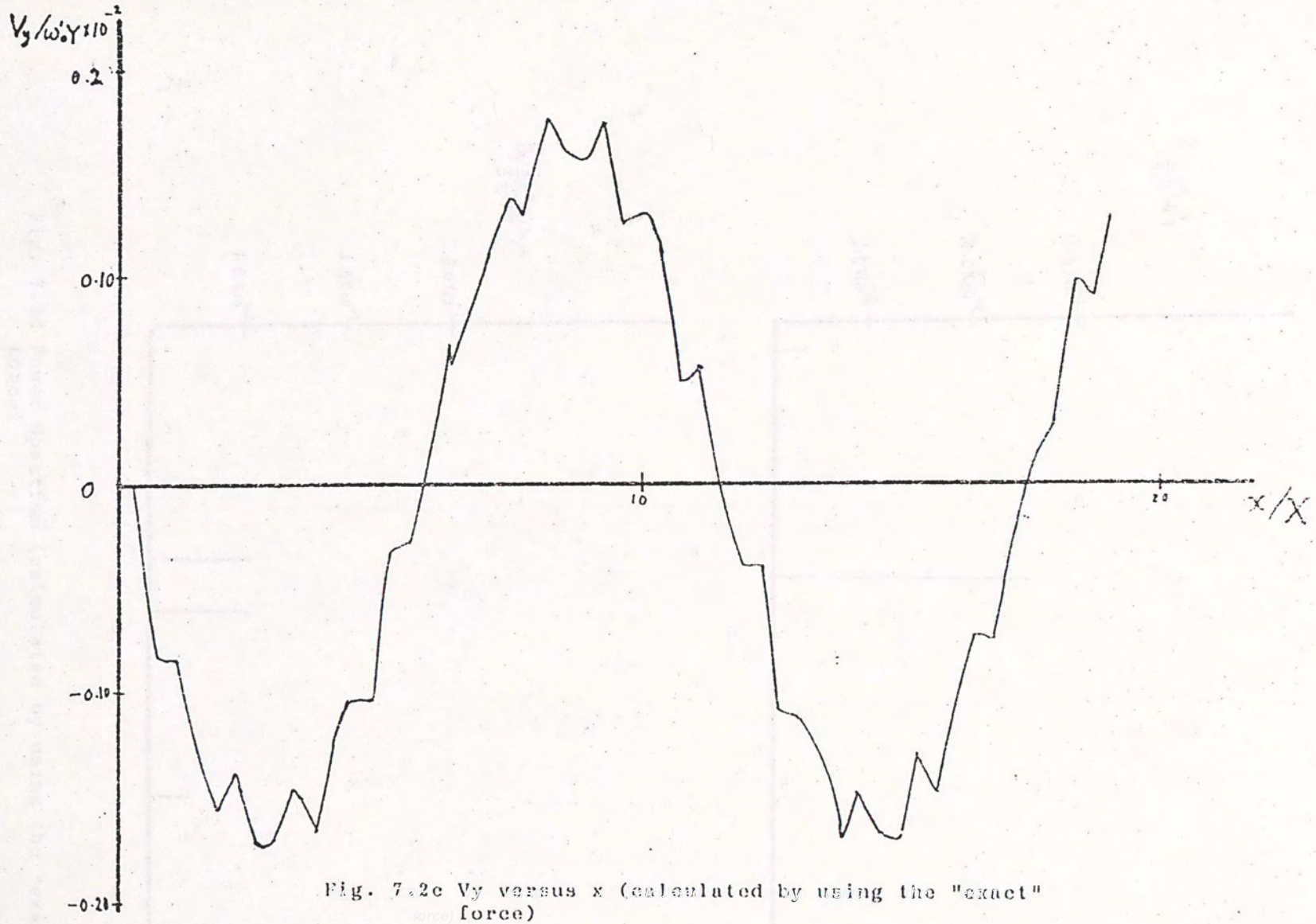

Fig. 7.2c Vy versus x (calculated by using the "exact" force)

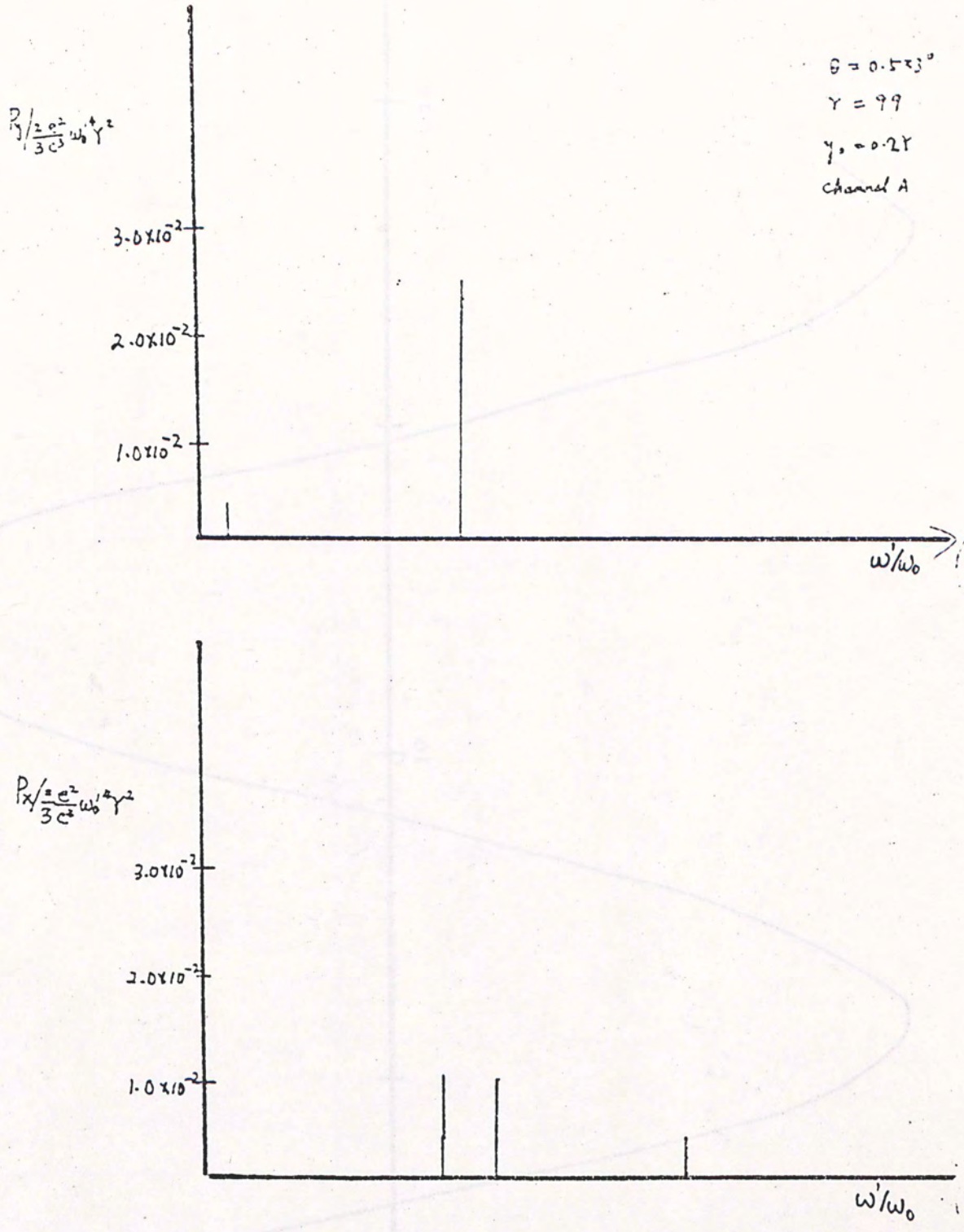

Fig. 7.2d Power spectrum (calculated by using the "exact" force)

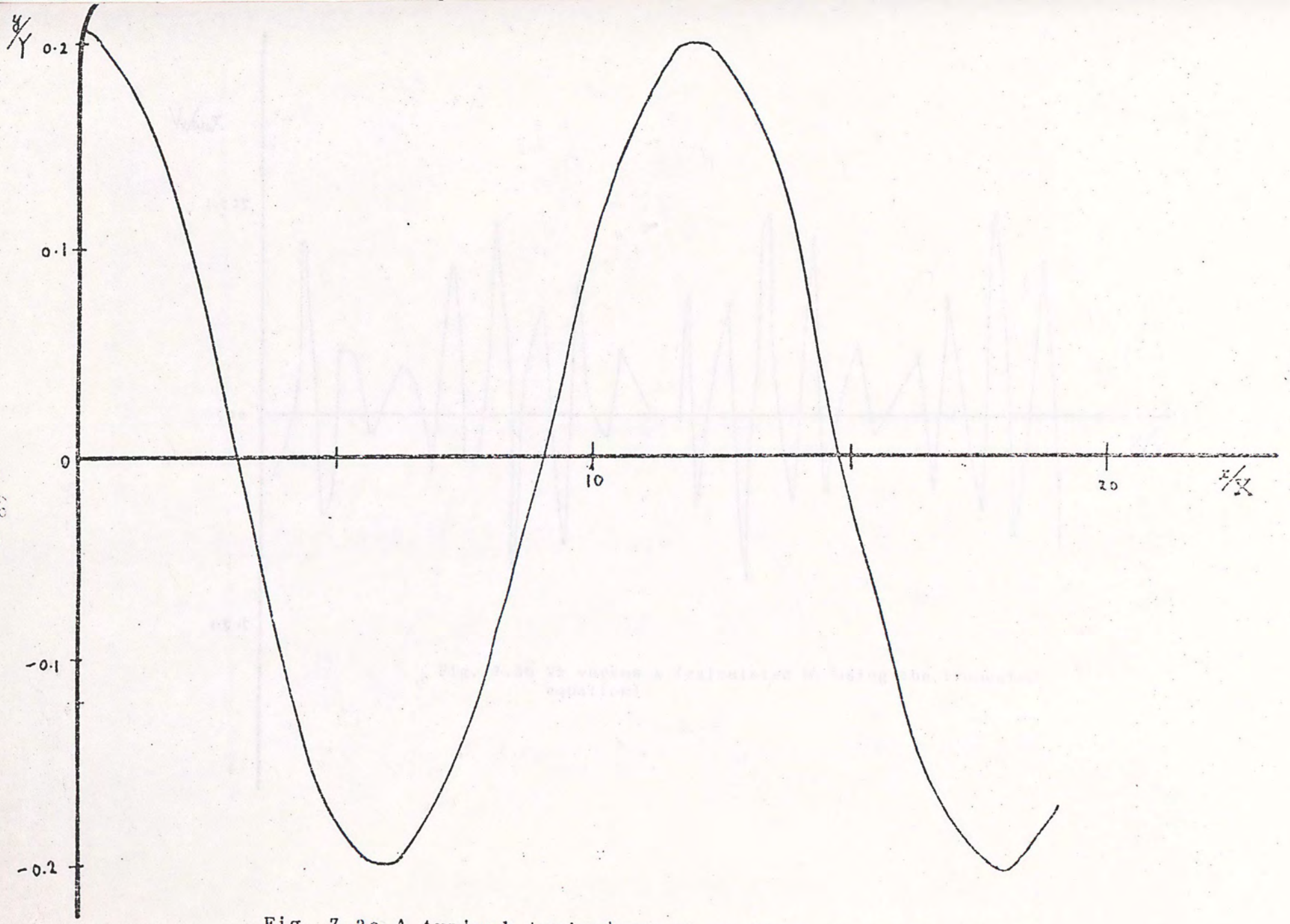

Fig. 7.3a A typical trajectory of positron along the {220} plane (calculated by using the truncated equation)

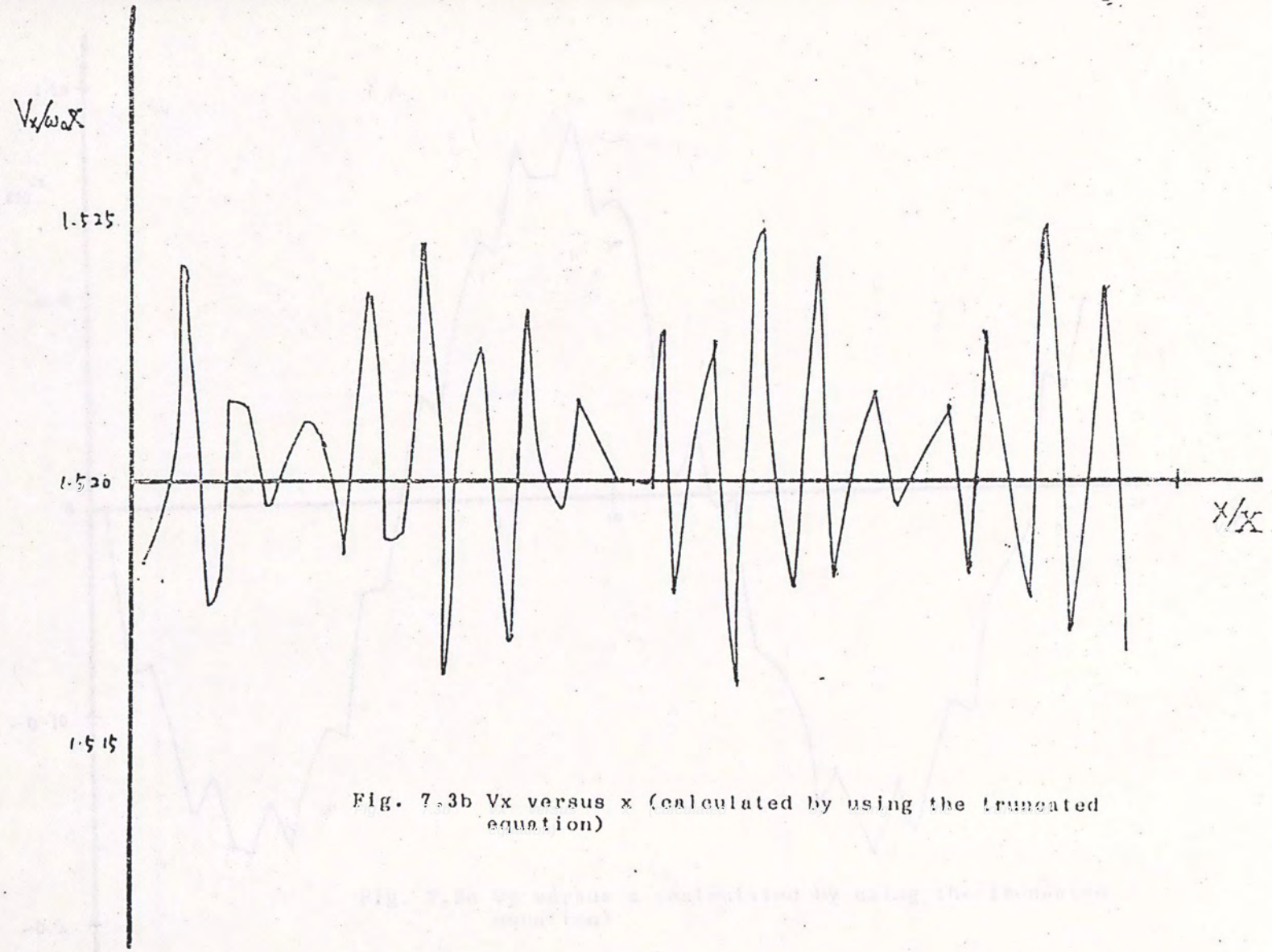

Fig. 7.3b Vx versus x (calculated by using the truncated equation)

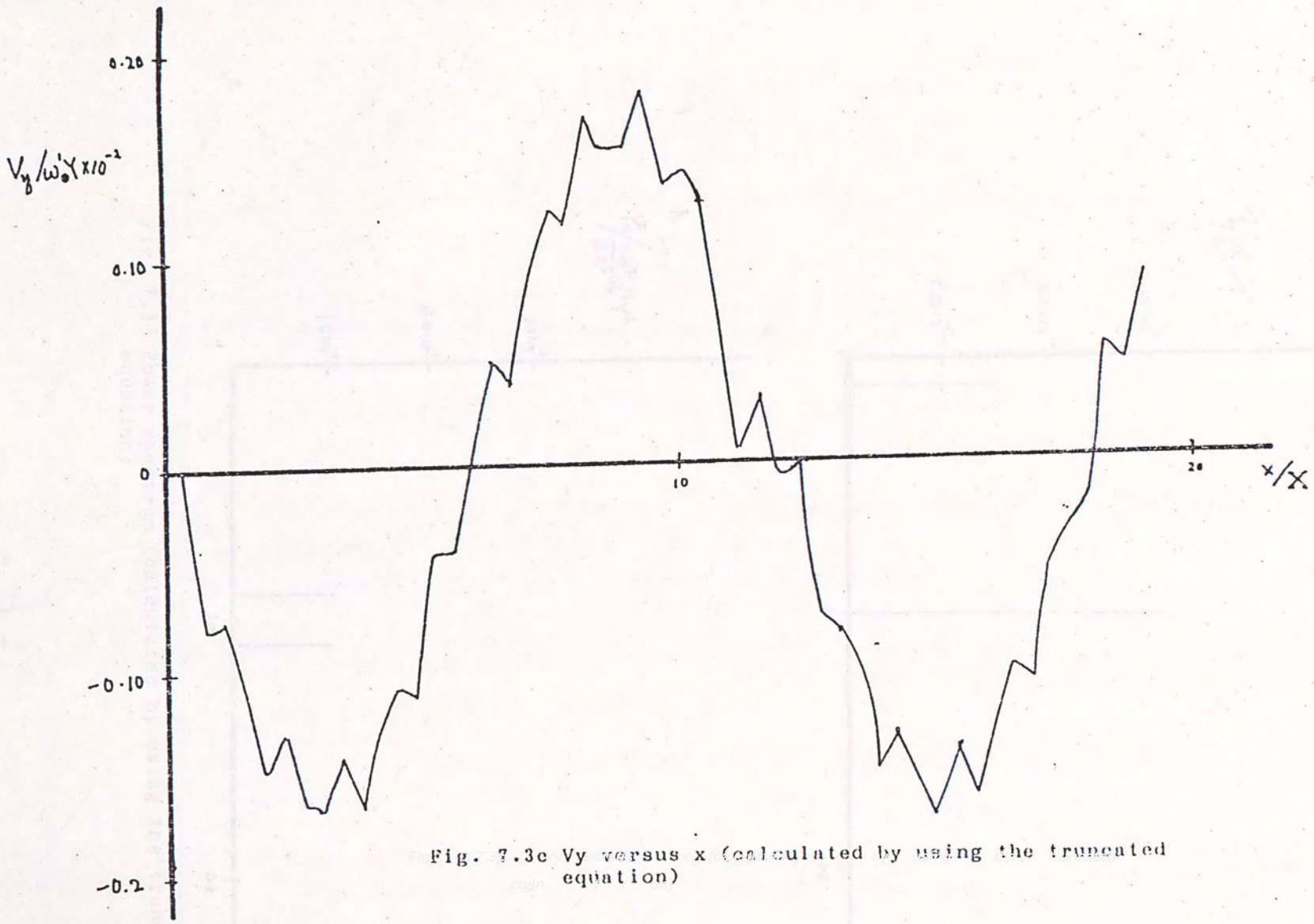

Fig. 7.3c Vy versus x (calculated by using the truncated equation)

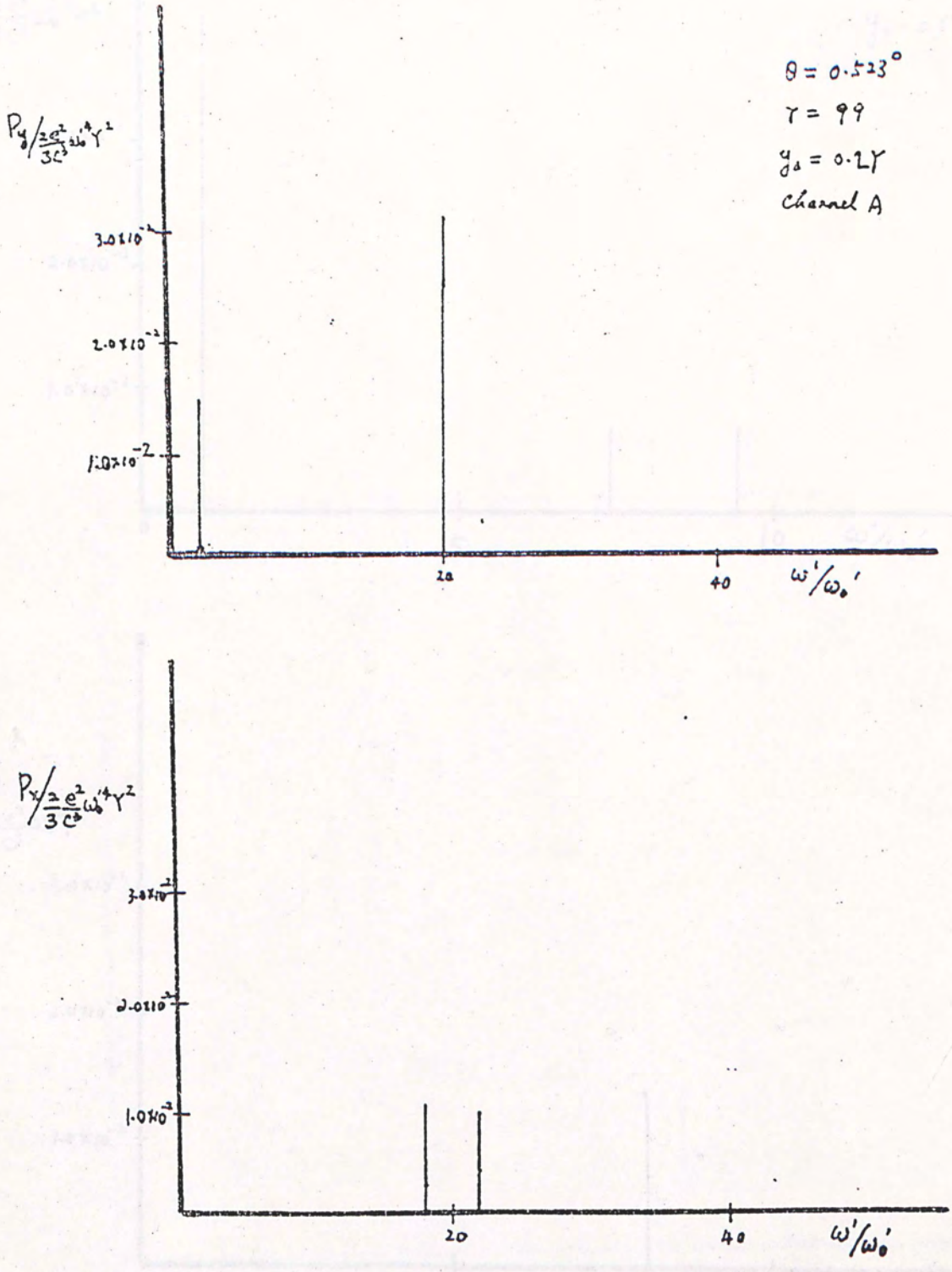

Fig. 7.3d Power spectrum (calculated by using the truncated equation)

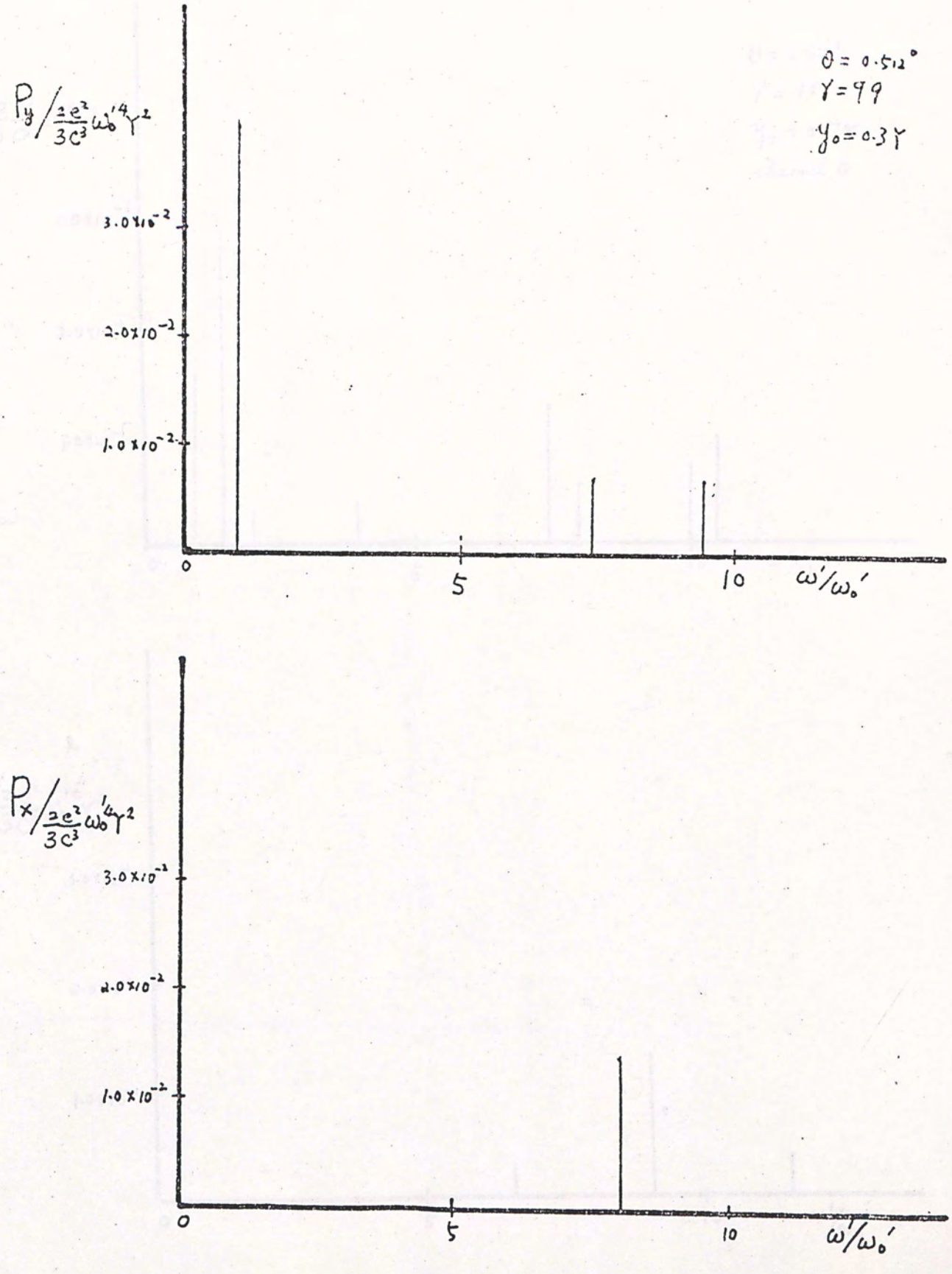

Fig. 7.4 Power spectrum of a symmetric channel

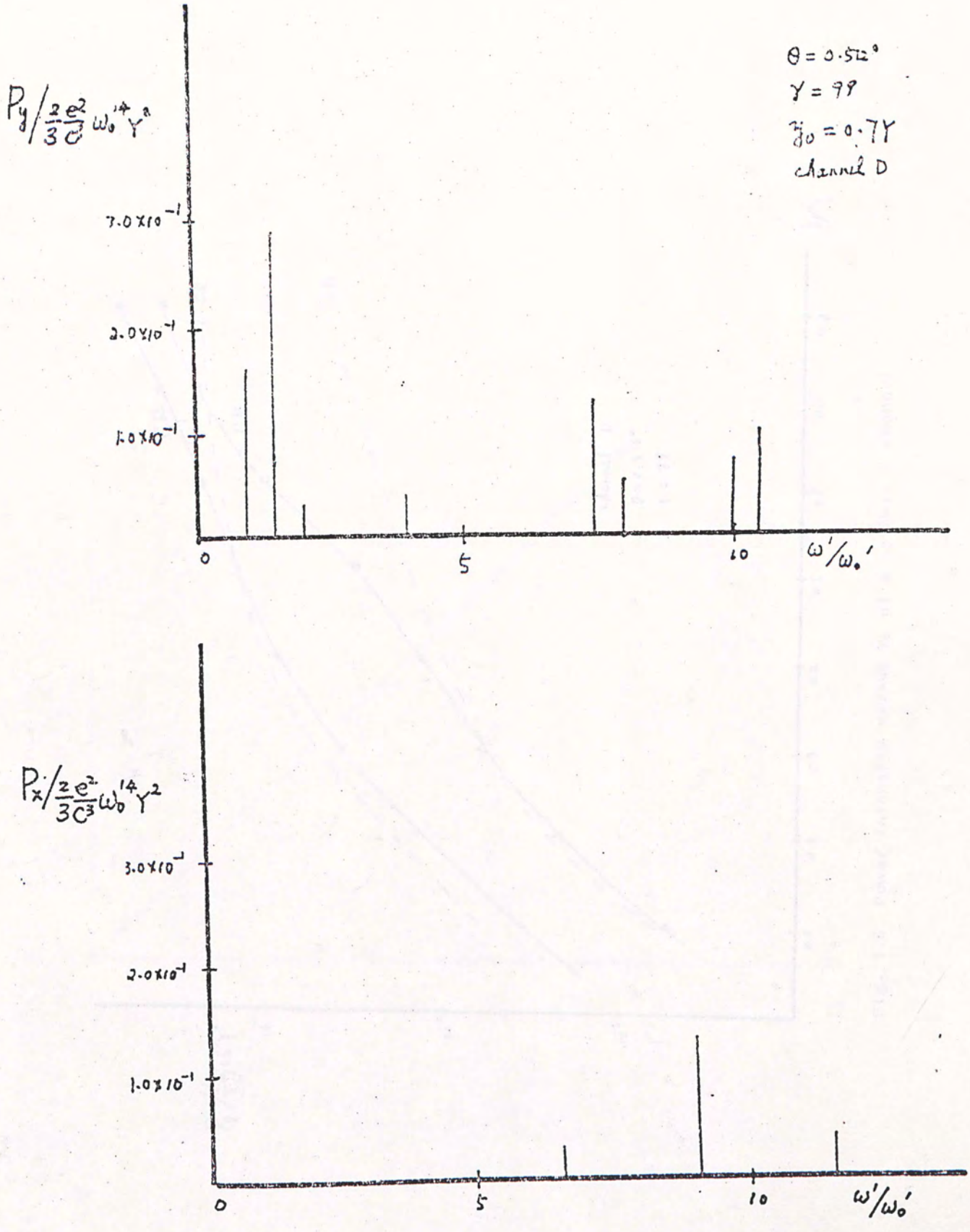

Fig. 7.5 Power spectrum of a symmetric channel with large-Y value

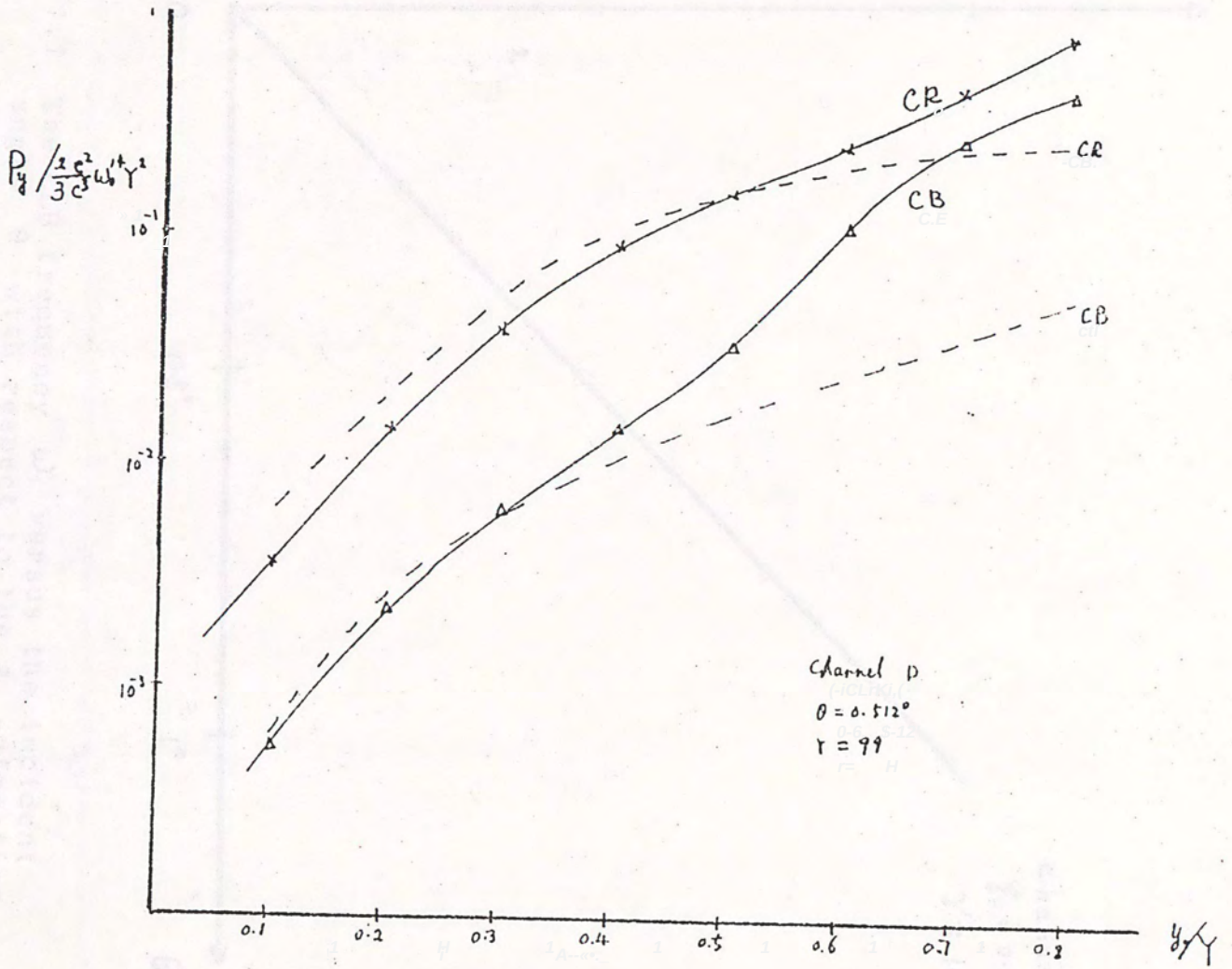

Fig. 7.6 Power intensity versus Y_0 of a symmetric channel

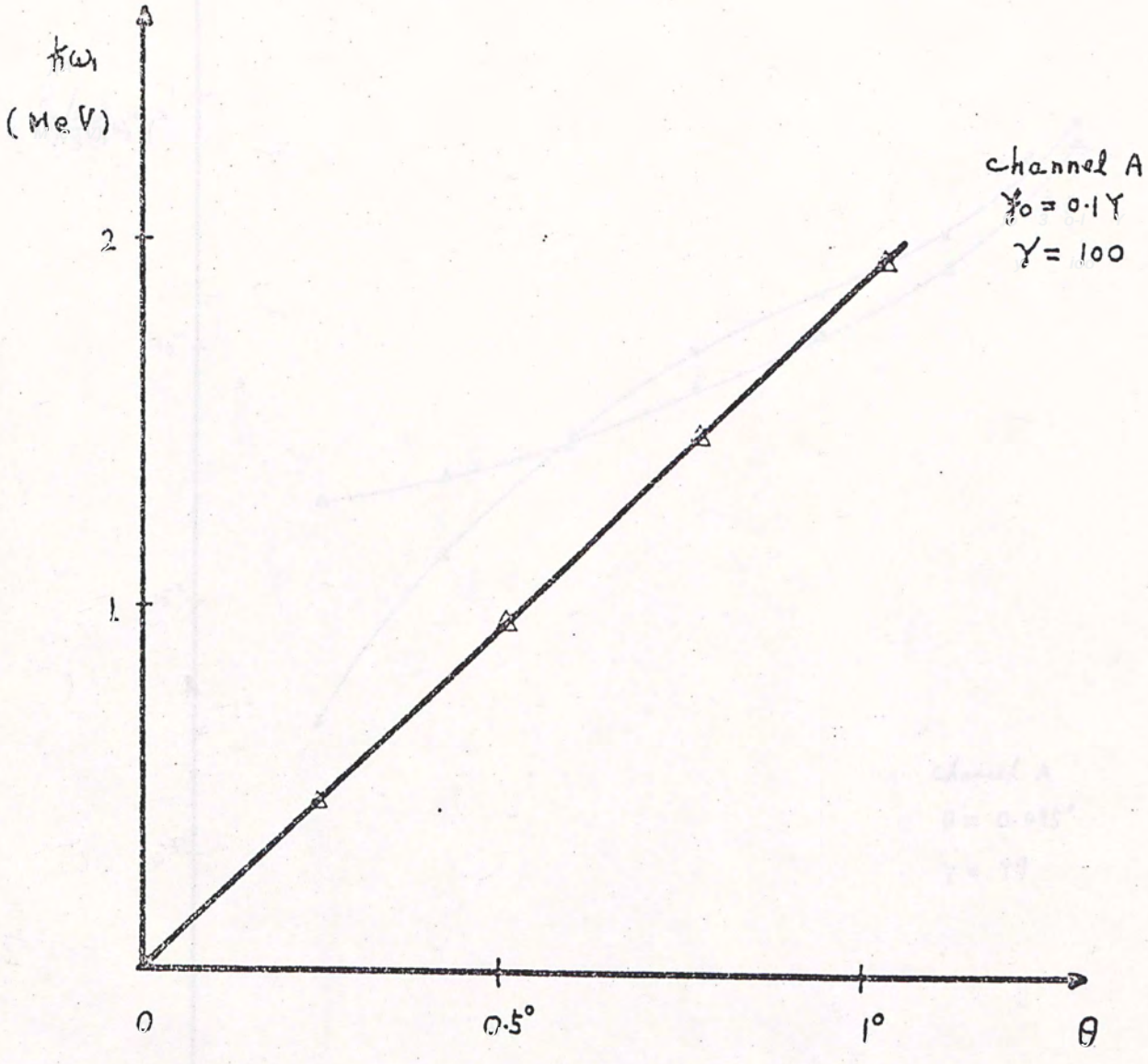

Fig. 7.7 The CLB frequency ω_1 versus the incident angle θ with respect to the z -direction

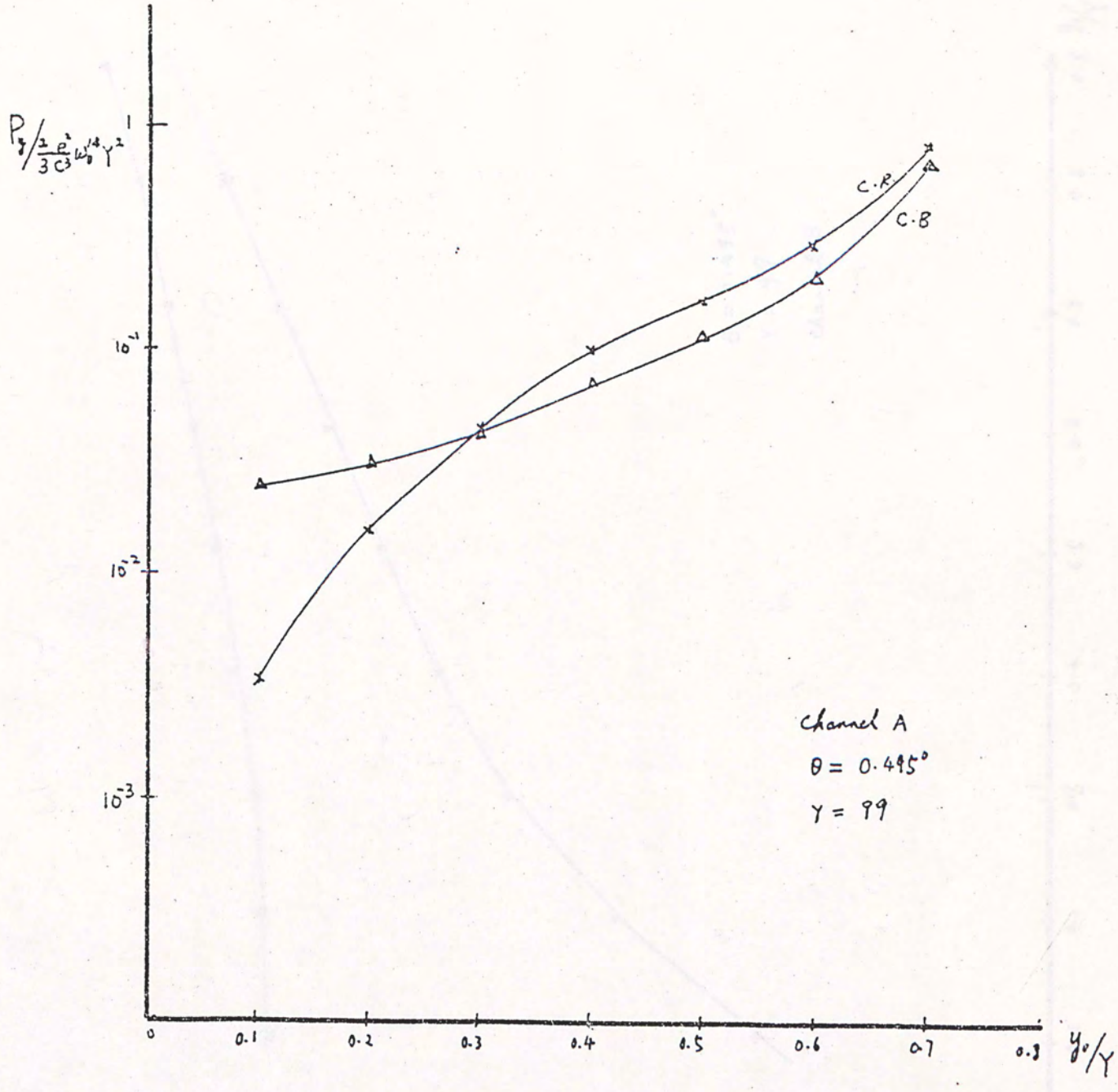

Fig. 7.8 Power intensity versus Y_o of Channel A (Antisymmetric channel)

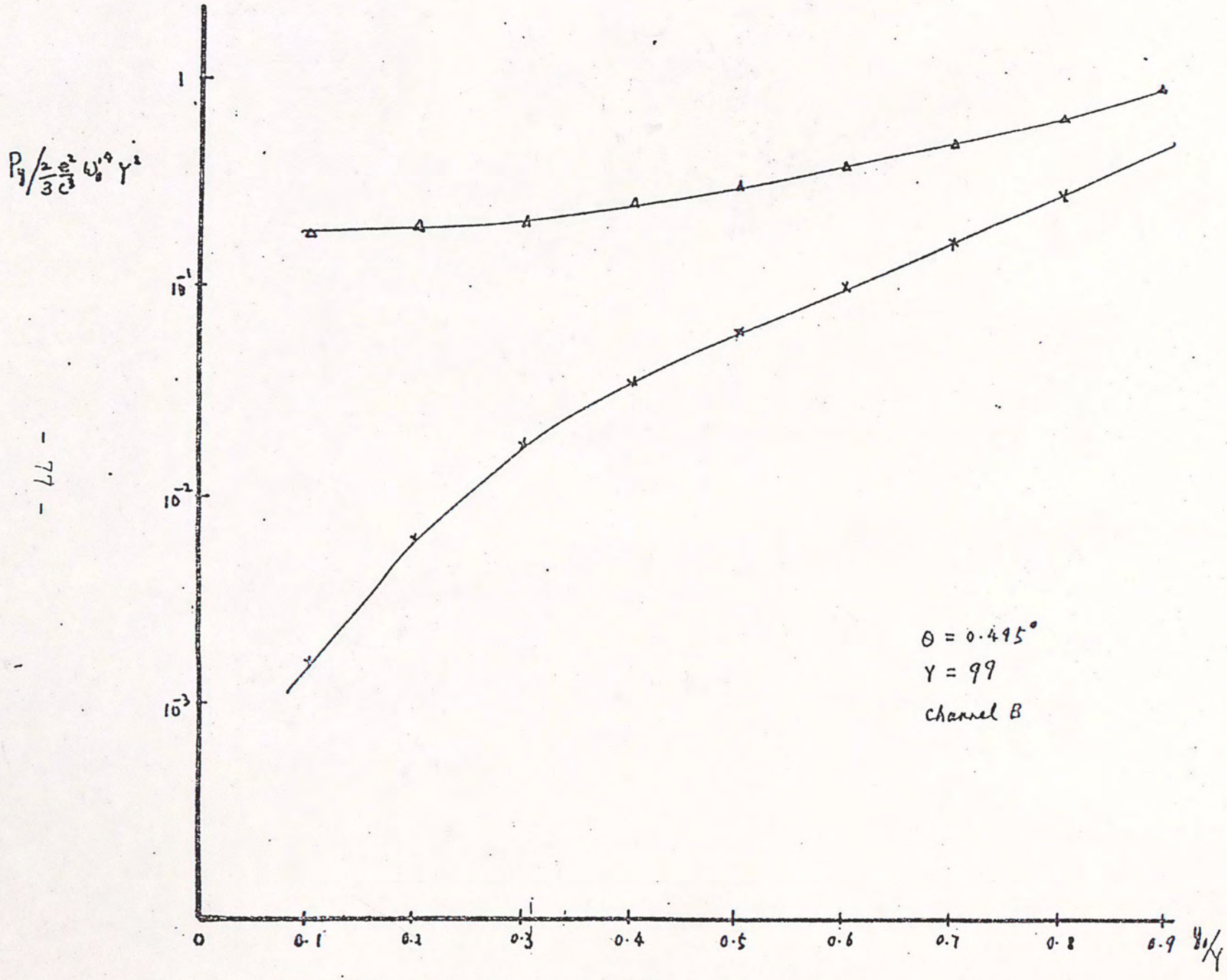

Fig. 7.9 Power intensity versus Y_0 of a narrow antisymmetric channel (channel B)